Ph.D. Thesis

Extracting the meson form factors from lattice QCD

Takashi Suzuki

suzuki@het.phys.sci.osaka-u.ac.jp

Osaka University Particle Physics Theory Group

February 9, 2016

Abstract

Precise computation of meson form factors in lattice QCD plays an important role in examining the standard model of particle physics. In this thesis, we study how to obtain a better control of three major systematic errors in the computation of the relevant three point functions to the form factors: finite lattice volume, finite lattice spacing, and violation of the chiral symmetry.

In part I, we focus on the finite volume effects on the pion form factors. Using chiral perturbation theory, we find ratios of correlators, which automatically cancel the dominant finite volume effects come from the zero-momentum mode of pions. We show that a precise extraction of the pion form factors can be carried out even on a rather small lattice size $L \sim 3$ fm.

In part II, we report on our recent numerical study in JLQCD collaboration about form factors of D meson semileptonic decays. We use the Möbius domain-wall fermions in order to reduce the systematic errors due to violation of chiral symmetry, as well as finite lattice spacing by simulating fine lattices. Our preliminary result for the semileptonic D meson form factors with the cutoff $1/a \sim 2.4$ GeV already shows a good agreement with the experiments.

Contents

1. INTRODUCTION

The standard model shows great successes as a fundamental theory of the particle physics. However, it does not explain everything perfectly, especially, the hierarchic mass spectrum (fine tuning problem), and existence of a theory beyond the standard model (BSM) is expected. Recently, the LHC experiments is running to research the BSM, but no definite evidence of the BSM has been reported so far.

Thus, a precise test of the standard model itself is becoming more and more important. Especially, precise analysis of hadron effects from theory side is awaited. Such an analysis however involves the strong interaction effects, which is described by the Quantum Chromodynamics (QCD) in the standard model, and requires non-perturbative calculation.

For such analysis, lattice QCD numerical simulation is an essential tool, since it enables us to calculate the strong interaction effects non-perturbatively from first principle. In fact, many topics of QCD physics, including hadron matrix elements, have been studied and developed by lattice QCD.

However, it should be noted that lattice QCD has inevitable three sources of systematic errors: finite lattice volume, finite lattice spacing, and violation of the chiral symmetry. Studying on these sources, we try to extract an accurate value of physical quantities. In this thesis, we study how to reduce these systematic errors on the meson form factors. In part I, we consider pion form factors, which are sensitive to the finite volume. In part II, we compute the D meson's form factors, which are sensitive to finite lattice spacings and violation of the chiral symmetry. These two parts are based on the following papers:

Part I : [1] H. Fukaya and T. Suzuki, Phys. Rev. D **90**, no. 11, 114508 (2014) doi:10.1103/PhysRevD.90.114508 [arXiv:1409.0327 [hep-lat]] (and also [2]).

Part II : PoS LATTICE 2015 (to be reported).

The latter article is a contribution by JLQCD collaboration to a conference proceedings, reporting on the preliminary results. We will submit a full paper after finalizing the analysis.

The rest of this thesis is organized as follows. Part I contains six sections: Secs. 2–7. First, Sec. 2 is an introduction to Part I. In Sec. 3, we review the ϵ expansion of chiral perturbation theory (ChPT) and present how to compute the correlators at one-loop level. In Sec. 4, we consider the two-point functions to illustrate our new idea. Then, our main

result for the pseudoscalar-vector-pseudoscalar three-point functions is presented in Sec. 5, including the NLO effects. In Sec. 6, we show how to extract pion vector form factors, and estimate the remaining finite volume effects numerically : we find that it is a few percent level already at $L = 3$ fm with a size of finite lattice volume L. Summary and conclusion of part I are given in Sec. 7.

Next, Part II contains Secs. 8–12 In Sec. 9, we explain our formula to calculate the form factors from lattice data. In Sec. 10, lattice set up of simulations we have used is summarized. Our numerical results are shown in Sec. 11. There, we determine the q^2 dependence of the form factors and compute the form factors at $q^2 = 0$. Summary and discussions of Part II are shown in Sec. 12.

Finally, we conclude this thesis in Sec. 13.

Part I

Finite volume effects on the pion form factors

2. INTRODUCTION TO PART I

In Part I, we consider the pion form factor in a finite volume, which is a main source of systematic errors on light hadron dynamics in lattice QCD. In particle physics, the finite volume effects are described by the propagation of the particles wrapping around finite lattice box. Since the pion is the lightest meson in QCD, the dominant part should come from the pion's propagation, $\exp(-m_\pi L)$. In the literature [5], it is often mentioned that $m_\pi L$ should be larger than 4 to suppress the finite volume effects to a level of a few percent. This means that a lattice simulation with a simulated pion mass at or below the physical point requires a large lattice size satisfying $L \gtrsim 6$ fm, which is still a challenging size for current computational resources. Especially, when we use a lattice fermion formulation such as domain-wall or overlap fermions to keep a good chiral symmetry, the available range of $m_\pi L$ is limited. Thus, it is important to find a way to control the finite volume effects even in a small lattice volume where $L \gtrsim 6$ fm is not satisfied.

Here we concentrate on the electro-magnetic form factor of pions. In contrast to the one-point and two-point functions [16–21], it is less known how much the finite volume effects affect on the three-point functions, which are relevant for the form factors. Experimentally, this form factor is related to the pion charge radius $\langle r^2 \rangle_V$ through the relation

$$\langle r^2 \rangle_V \;=\; 6 \frac{dF_V(q^2)}{dq^2}\bigg|_{q^2=0}, \tag{1}$$

where $F_V(q^2)$ denotes the electro-magnetic form factor at the momentum transfer q^2. In terms of ChPT, it is related to the low-energy constant L_9 (or l_6 in the $SU(2)$ case), which appears at the next-to-leading order (NLO) in the chiral Lagrangian [8, 9].

However, the lattice results for the pion charge radius have showed a sizably lower value than the experimental value $\langle r^2 \rangle_V = 0.452(11)$ fm^2 [10] (the recent lattice results are summarised in [11]). It is only recently that consistent values of $\langle r^2 \rangle_V$ were reported by simula-

tions near the physical point [12–14]. According to ChPT, it is known that the pion charge radius shows a logarithmic divergence as the pion mass goes to zero. Thus, we may recognize that our simulated pion masses are too large to reproduce the logarithmic divergence, unless we directly simulate QCD near the chiral limit $m_\pi \to 0$. Namely, in order to examine the chiral logarithm of the pion charge radius, it is essential to simulate lattice QCD in the very vicinity of the chiral limit. In this region, above condition $m_\pi L > 4$ is quite severe, and how to control the finite volume effects becomes more important.

We would like to therefore find a way to control the finite volume effects even in a small lattice volume. Here we notice that the naive criterion about $m_\pi L$ mentioned above comes from the fact that the pion's zero-momentum mode gives the dominant finite volume effects. The pion's zero-momentum mode can propagate wrapping around the lattice volume and gives a contribution naively estimated as $\exp(-m_\pi L)$. While, such contribution from the excited pion states with an energy E_π is a much smaller, $e^{-E_\pi L} < 1.87 \times 10^{-3}$, since their discrete energy satisfy $E_\pi > 2\pi/L$ (or equivalently $E_\pi L > 2\pi$) in a finite volume. We can therefore expect that the finite volume effects can be well controlled by eliminating or reducing the dominant contribution from the pion's zero-momentum mode. If this expectation is true, we can extract a reliable result for physical quantities from lattice simulation on a small volume where $m_\pi L > 4$ is not satisfied and the finite volume effects is generally large.

In order to find good observables which cancel contributions from the pion's zero-momentum mode, we use the so-called ϵ expansion of ChPT [6, 7], which treats the pion's zero-momentum mode separately and non-perturbatively. The ϵ expansion is valid even when the Compton wavelength of pions exceeds a lattice size: $m_\pi L < 1$. In this case, corrections from the finite volume effects is generally $\sim 100\%$, and the lattice data is largely contaminated by the finite volume effects. In the previous works, the ϵ expansion of ChPT was mainly used to extract the low-energy constants [16–21], using a bunch of Bessel functions which appears as a special feature of the ϵ expansion, and to calculate one or two point functions except for [22, 23].

In our work [1], we compute the pseudoscalar-vector-pseudoscalar three point function within the ϵ expansion of ChPT to extract the electro-magnetic form factors.

We find a way to automatically cancel the dominant part of the finite volume effects. Since the zero-momentum contribution does not depend on space-time, two simple steps are enough to achieve this:

1. inserting non-zero momenta to relevant operators (or taking a subtraction of the correlators at different source points when one or two of the inserted momenta are zero).

2. taking ratios of them.

We also compute the NLO corrections and show that these effects are actually suppressed by $1/F^2L^2$, where F denotes the pion decay constant.

Here we would like to emphasize a feature of our new approach. As mentioned above, our strategy is to cancel the dominant finite volume effects which comes from the zero momentum mode of pions and is written in terms of the Bessel functions. This approach is different from that of the previous works where they *use* Bessel functions to extract the low-energy constants. In particular, it is important to note that there is essentially no need to use Bessel functions in our method. Moreover, since the dominance of the zero momentum mode of pions is universal, we expect a wide application of our method. It may be useful for higher correlation functions of any operators or for the conventional p regime.

A part of our result has been already applied to numerical works by JLQCD collaboration [13, 14] where they simulate QCD at a very small pion mass in a small volume. They reported a higher value for the pion charge radius than the experimental value confirming the strong chiral logarithmic enhancement.

3. THE ϵ EXPANSION OF CHPT

In this section, we introduce the ϵ expansion of ChPT, and explain how to calculate correlation functions up to one-loop level. First, we show the counting rule of the ϵ expansion. Second, we give the chiral lagrangian with pseudo-scalar and vector source terms, and provide a general procedure of calculation of correlation functions from a partition function. Finally, we explain the technical details of our calculation in the ϵ expansion at the end of this section.

3–a. The chiral Lagrangian

We consider N_f-flavor ChPT in an Euclidean finite volume $V = TL^3$ with the periodic boundary condition in every direction, where T denotes a size of lattice volume in temporal

direction. The Lagrangian [8, 9] is given by

$$\mathcal{L}_{\rm ChPT} = \frac{F^2}{4}{\rm Tr}\left[\left(\partial_\mu U(x)\right)^\dagger\left(\partial_\mu U(x)\right)\right] - \frac{\Sigma}{2}{\rm Tr}\left[\mathcal{M}^\dagger U(x) + U^\dagger(x)\mathcal{M}\right] + \cdots, \tag{2}$$

where $U(x)$ denote the chiral field which is an element of the group $SU(N_f)$. F is the pion decay constant and Σ is the chiral condensate both in the chiral limit. The ellipses denote the terms at the higher orders. For simplicity, we set the quark mass matrix $\mathcal{M}$ to be degenerate and diagonal: $\mathcal{M} = {\rm diag}(m, m, m, \cdots)$.

As we have mentioned in Sec. 2, we would like to consider the finite volume effects in a small lattice where $m_\pi L > 4$ is not satisfied. Especially, in the $m_\pi L < 1$ case, which is the so-called ϵ regime [6], one has to take special care about the pion's zero-momentum mode. In this extreme regime, the vacuum has non-perturbatively large fluctuations and become the dynamical variables. Namely, one must integrate the pion's zero-momentum mode exactly. Thus, it is useful to separate the zero-momentum mode from the non-zero momentum modes and parametrize the chiral field as

$$U(x) = U_0\,\exp\left(\frac{i\sqrt{2}}{F}\xi(x)\right), \quad U_0 \in SU(N_f), \tag{3}$$

where U_0 denotes the zero-momentum modes. The non-zero momentum mode can be decomposed as $\xi(x) = T^a\xi^a(x)$ with $SU(N_f)$ generators T^a with the normalization of ${\rm Tr}[T^aT^b] = \frac{1}{2}\delta^{ab}$. Since the zero-modes U_0 are separated from $\xi(x)$ fields, a constraint

$$\int d^4x\,\xi(x) = 0, \tag{4}$$

must be satisfied to keep from the double-counting of the zero-modes.

Now, we would like to rewrite the chiral Lagrangian Eq. (2) in terms of the ϵ expansion according to the counting rule given by

$$\begin{aligned}&\mathcal{O}(1) : U_0,\\ &\mathcal{O}(\epsilon) : \partial_\mu,\ \frac{1}{V^{1/4}},\ m_\pi^{1/2},\ m^{1/4},\ \xi(x),\end{aligned} \tag{5}$$

as

$$\begin{aligned}\mathcal{L}_{\rm ChPT} \;=\; &-\frac{\Sigma}{2}{\rm Tr}\left[\mathcal{M}^\dagger U_0 + U_0^\dagger\mathcal{M}\right] + \frac{1}{2}{\rm Tr}\left[\partial_\mu\xi\partial_\mu\xi\right](x)\\ &+\frac{\Sigma}{2F^2}{\rm Tr}\left[\left(\mathcal{M}^\dagger U_0 + U_0^\dagger\mathcal{M}\right)\xi^2\right](x) + \cdots.\end{aligned} \tag{6}$$

This Lagrangian describes a hybrid system of a matrix U_0 and bosonic $\xi(x)$ fields with weakly interacting. The counting rule Eq. (5) means that zero-momentum mode U_0 is treated non-perturbatively and other quantities are treated as perturbative small quantity of $\mathcal{O}(\epsilon)$. In the ϵ expansion, $1/V^{1/4}$ and $m_\pi^{1/2}$ are regarded as a same order quantity. This reflects that the ϵ expansion is valid in a region $m_\pi L < 1$. Especially, non-zero momentum modes $\xi(x)$ are treated as perturbative quantity with the same order of $1/V^{1/4}$. This can be recognized from the propagator of ξ fields (see Eq. (7)).

It is not difficult to perform the Gaussian integrals for $\xi(x)$ fields. Thus, we use the correlator in quark-line basis,

$$\langle [\xi(x)]_{ij} [\xi(y)]_{kl} \rangle_\xi \;=\; \delta_{il}\delta_{jk}\bar{\Delta}(x-y) - \delta_{ij}\delta_{kl}\frac{1}{N_f}\bar{\Delta}(x-y), \tag{7}$$

where the second term reflects the constraint $\mathrm{Tr}\xi = 0$, and

$$\bar{\Delta}(x) \;\equiv\; \frac{1}{V}\sum_{p\neq 0}\frac{e^{ipx}}{p^2}, \tag{8}$$

describes the propagator of the massless bosons. The index in summation runs over the non-zero 4-momentum $p = 2\pi(n_t/T, n_x/L, n_y/L, n_z/L)$, with integers n_μ, except for $p = (0,0,0,0)$, which comes from the constraint Eq. (4).

While $\xi(x)$ fields can be treated perturbatively, the zero-momentum mode denoted by U_0 must be integrated non-perturbatively (we denote it by $\langle \cdots \rangle_{U_0}$ defined in Eq. (48)). These matrix integrals gives the expression in term of the Bessel functions [24–26], which is a feature of the ϵ regime. Historically, this peculiar feature is used for extracting Σ, the leading LEC's, and F, which are more sensitive to the volume than others. However, for the other LEC's at NLO, we should take a different way, or should remove the effects from the finite size. In this study on the vector form factor of pions, which is related to the L_9 among the LEC's, the zero-momentum mode integration plays a less important role.

3–b. Partition function and correltors

In this subsection, we consider the partition function of ChPT in the ϵ regime and show how to calculate the correlation functions. First, we introduce the relevant source terms to the chiral Lagrangian Eq. (2). Since the Lagrangian is invariant under the chiral rotation,

$$U(x) \to g_L U(x) g_R^\dagger, \quad g_L, g_R \in SU(N_f), \tag{9}$$

the vector or axial vector operators are given through the Noether's theorem for the vectorlike transformation $g_L = g_R$ and the axial one $g_L = g_R^\dagger$. It is easy to see that adding these operators is equivalent to replacing the derivatives by the "covariant" derivatives:

$$\partial_\mu \to \nabla_\mu U(x) \equiv \partial_\mu U(x) - i(v_\mu(x) + a_\mu(x))U(x) + iU(x)(v_\mu(x) - a_\mu(x)), \tag{10}$$

where $v_\mu(x)$ and $a_\mu(x)$ denote the vector and axial-vector sources, respectively. Similarly, since the Lagrangian is invariant under the Parity transformation,

$$U(x) \to U^\dagger(x), \quad x = (t, x, y, z) \to x = (t, -x, -y, -z), \tag{11}$$

adding a scalar $U(x) + U^\dagger(x)$ and a pseudoscalar $U(x) - U^\dagger(x)$ is absorbed in the mass matrix:

$$\mathcal{M} \to \mathcal{M}_J \equiv \mathcal{M} + s(x) + ip(x), \tag{12}$$

where $s(x)$ and $p(x)$ denote the scalar and pseudoscalar sources, respectively. We set $s(x) = a_\mu(x) = 0$ in the following, since it is not necessary in our calculations.

Next, let us introduce the NLO terms of the chiral lagrangian. However, some of them are irrelevant to our calculations. In this study, it is enough to consider the terms with the low-energy constants L_i $(i = 4, \cdots 9)$. Namely, we consider the Lagrangian

$$\begin{aligned}
\mathcal{L}(s, p, v_\mu, a_\mu) \;=\; & \frac{F^2}{4}\mathrm{Tr}[\nabla_\mu U^\dagger(x)\nabla_\mu U(x)] - \frac{\Sigma}{2}\mathrm{Tr}[\mathcal{M}_J^\dagger U(x) + U^\dagger(x)\mathcal{M}_U] \\
& + L_4\frac{2\Sigma}{F^2}\mathrm{Tr}[(\nabla_\mu U(x))^\dagger \nabla_\mu U(x)] \times \mathrm{Tr}[\mathcal{M}_J^\dagger U(x) + U^\dagger(x)\mathcal{M}_J] \\
& + L_5\frac{2\Sigma}{F^2}\mathrm{Tr}\left[(\nabla_\mu U(x))^\dagger \nabla_\mu U(x)(\mathcal{M}_J^\dagger U(x) + U^\dagger(x)\mathcal{M}_J)\right] \\
& - L_6\left(\frac{2\Sigma}{F^2}\mathrm{Tr}[\mathcal{M}_J^\dagger U(x) + U^\dagger(x)\mathcal{M}_J]\right)^2 \\
& - L_7\left(\frac{2\Sigma}{F^2}\mathrm{Tr}[\mathcal{M}_J^\dagger U(x) - U^\dagger(x)\mathcal{M}_J]\right)^2 \\
& - L_8\left(\frac{2\Sigma}{F^2}\right)^2 \mathrm{Tr}[\mathcal{M}_J^\dagger U(x)\mathcal{M}_J^\dagger U(x) + U^\dagger(x)\mathcal{M}_J U^\dagger(x)\mathcal{M}_J] \\
& + iL_9\mathrm{Tr}[F_{\mu\nu}^R(x)\nabla^\mu U(x)(\nabla^\nu U(x))^\dagger + F_{\mu\nu}^L(x)(\nabla^\mu U(x))^\dagger \nabla^\nu U(x)],
\end{aligned} \tag{13}$$

where

$$\begin{aligned}
F_{\mu\nu}^I(x) \;&=\; \partial_\mu F_\nu^I(x) - \partial_\nu F_\mu^I(x) - i[F_\mu^I(x), F_\nu^I(x)], \qquad I = R, L, \\
F_\mu^R(x) \;&=\; v_\mu(x) + a_\mu(x), \qquad F_\mu^L(x) = v_\mu(x) - a_\mu(x).
\end{aligned} \tag{14}$$

The calculation of ChPT is performed in the functional integral formalism. The partition function is defined by

$$\mathcal{Z}(s,p,v_\mu,a_\mu) = \int \prod_x dU(x) \exp\left[-\int d^4x \mathcal{L}(s,p,v_\mu,a_\mu)\right], \tag{15}$$

and the correlation functions are computed by differentiating it with respect to the corresponding sources, and take their zero limits. The pseudoscalar two-point function, for example, is given by

$$\langle P^a(x)P^b(y)\rangle \;=\; \frac{1}{\mathcal{Z}(0,0,0,0)}\frac{\delta}{\delta p^a(x)}\frac{\delta}{\delta p^b(y)}\mathcal{Z}(s,p,v_\mu,a_\mu)\Big|_{s,p,v_\mu,a_\mu=0}, \tag{16}$$

where $p^a(x)$ denotes the coefficient of an $SU(N_f)$ generator T^a, where we decompose the source as $p(x) = T^a p^a(x)$.

One should note that our non-trivial parametrization of $U(x)$ needs a non-trivial Jacobian in the functional integration measure:

$$\int \prod_x dU(x) \;=\; \int dU_0 \prod_x d\xi(x) \mathcal{J}(U_0,\xi). \tag{17}$$

A perturbative calculation [16, 29] has shown

$$\mathcal{J}(U_0,\xi) \;=\; \exp\left(-\int d^4x \frac{N_f}{3F^2V}\mathrm{Tr}\;\xi^2(x) + \mathcal{O}(\epsilon^4)\right), \tag{18}$$

which can be regarded as an additional mass term of the $\xi(x)$ fields at the one-loop level. Note that this additional mass does not vanish even in the $m \to 0$ limit, which keeps the theory infra-red finite.

Finally, let us consider the θ vacuum and fixing topology. In the ϵ regime, we often consider a fixed topological sector, rather than the full QCD vacuum with the vacuum angle $\theta = 0$. For this purpose, we encode the non-zero vacuum angle θ to the mass term [30],

$$\mathcal{M} \to \mathcal{M}_\theta = \mathcal{M}\exp(-i\theta/N_f), \tag{19}$$

using the axial $U(1)_A$ rotation. Then we can perform a Fourier transformation with respect to θ to obtain the partition function at fixed topology,

$$\mathcal{Z}^Q(s,p,v_\mu,a_\mu) \equiv \int_0^{2\pi} \frac{d\theta}{2\pi}\left[e^{i\theta Q}\mathcal{Z}(s,p,v_\mu,a_\mu)\big|_{\mathcal{M}=\mathcal{M}_\theta}\right], \tag{20}$$

where Q denotes the topological charge of the original gauge fields. It is known that this θ integral can be absorbed in the group integration of the zero-momentum mode: redefining the zero-momentum mode,

$$e^{i\theta/N_f}U(x) \;=\; \overline{U}_0 \exp\left(\frac{i\sqrt{2}}{F}\xi(x)\right), \tag{21}$$

where $\overline{U_0} \in U(N_f)$, the zero-momentum mode part of the functional integral is modified to

$$\int \frac{d\theta}{2\pi}\exp(i\theta Q)\int_{SU(N_f)} dU_0 F(\mathcal{M}^\dagger e^{i\theta/N_f}U_0) = \int_{U(N_f)} d\overline{U}_0 (\det \overline{U}_0)^Q F(\mathcal{M}^\dagger \overline{U}_0), \tag{22}$$

where we have used the fact that the zero-momentum mode in the Lagrangian always appears as a function of $\mathcal{M}^\dagger e^{i\theta/N_f}U_0$ (and its Hermitian conjugate). Fixing the topology is technically easier since the $U(N_f)$ group integral is simpler than that of $SU(N_f)$. It is also useful for investigating the finite volume physics which is sensitive to the topology of the gauge fields. It is important to note that the fixing topology effect is totally encoded in the pion's zero-momentum mode, and therefore, is automatically eliminated once the effect of the zero-momentum mode is eliminated. Since we will be able to cancel the effect of U_0 (from the LO contribution), in the following sections, we do not distinguish U_0 and $\overline{U}_0$ unless explicitly stated.

We are now ready for the 1-loop computations. However, we would like to give some useful technical details which simplify the calculations, in the next subsection.

3–c. Technical details

Because of the non-trivial parametrization of the chiral field, we have a lot of diagrams to be computed in the ϵ expansion of ChPT even at NLO. Here we rewrite the Lagrangian using the non-self-contracting (NSC) vertices, and compute some of 1-loop diagrams in advance, as corrections to the chiral Lagrangian. This reduces the number of diagrams and simplify our calculation.

The n-point NSC vertex is defined by

$$[\xi^n(x)]^{NSC} \;\equiv\; \xi^n(x) - (\text{all possible } \xi \text{ contractions}). \tag{23}$$

and we can absorb the contracted part in the redefinition of the lower dimensional terms in the Lagrangian. Note that $\langle[\xi^n(x)]^{NSC}\rangle_\xi = 0$ by definition. For example, a term in the

Lagrangian at NLO can be re-expressed by

$$\frac{1}{6F^2}\mathrm{Tr}[\partial_\mu\xi\xi\partial_\mu\xi\xi - \xi^2(\partial_\mu\xi)^2] \;=\; \frac{1}{6F^2}\mathrm{Tr}[\partial_\mu\xi\xi\partial_\mu\xi\xi - \xi^2(\partial_\mu\xi)^2]^{NSC} + \frac{1}{2}\mathrm{Tr}\left[(\partial_\mu\xi)^2\right]\Delta Z^\xi + \frac{1}{2}\mathrm{Tr}\left[\xi^2\right]\Delta M^2, \tag{24}$$

where

$$\Delta M^2 \;=\; -\frac{N_f}{3F^2}\partial_\mu^2\bar{\Delta}(0) = \frac{N_f}{3F^2V}, \tag{25}$$

can be absorbed in the re-definition of the mass term, and

$$\Delta Z^\xi \;=\; -\frac{N_f}{3F^2}\bar{\Delta}(0), \tag{26}$$

can be absorbed in the re-definition of the kinetic term. Here, and in the following, the momentum summations in embeded in $\bar{\Delta}(0)$ etc. are kept unperformed until the very end of the calculation, except for the trivially clear cases like $\partial_\mu^2\bar{\Delta}(0) = -1/V$, $\partial_\mu\bar{\Delta}(0) = 0$. In this work, we employ the dimensional regularization for the loop integrals.

With the NSC vertices, the action is expanded as

$$\mathcal{S}_{\mathrm{ChPT}} \;=\; \int d^4x\,\mathcal{L} = \mathcal{S}^{\mathrm{LO}} + \mathcal{S}^{\mathrm{NLO}} + \mathcal{S}^{\mathrm{src}} + \cdots, \tag{27}$$

where

$$\mathcal{S}^{\mathrm{LO}} \;=\; -\frac{Z^\Sigma\Sigma V}{2}\mathrm{Tr}[\mathcal{M}^\dagger U_0 + U_0^\dagger\mathcal{M}] + \int d^4x\left\{\frac{1}{2}\mathrm{Tr}[\partial_\mu\xi\partial^\mu\xi](x)\right\}(Z^\xi)^2, \tag{28}$$

$$\mathcal{S}^{\mathrm{NLO}} \;=\; \mathcal{S}_K^{\mathrm{NLO}} + \mathcal{S}_M^{\mathrm{NLO}},$$

$$\mathcal{S}^{\mathrm{src}} \;=\; \int d^4x\mathrm{Tr}\left[p(x)P(x) + v_\mu(x)V^\mu(x)\right], \tag{29}$$

where

$$\mathcal{S}_K^{\mathrm{NLO}} \;\equiv\; \int d^4x\frac{1}{6F^2}\mathrm{Tr}[\partial_\mu\xi\xi\partial^\mu\xi\xi - \xi^2\partial_\mu\xi\partial^\mu\xi]^{NSC}(x), \tag{30}$$

$$\mathcal{S}_M^{\mathrm{NLO}} \;\equiv\; \int d^4x\frac{\Sigma}{2F^2}\mathrm{Tr}\left[\left(\mathcal{M}^\dagger U_0 + U_0^\dagger\mathcal{M} + \frac{N_f}{\Sigma V}\right)\xi^2\right]^{NSC}(x). \tag{31}$$

Note that the linear term in $\xi(x)$ disappears because of the constraint Eq. (4).

Here, the source operators are given by

$$
\begin{aligned}
P(x) \;=\;& iZ^{P1}\frac{\Sigma}{2}[U_0 - U_0^\dagger] - Z^{P2}\frac{\Sigma}{\sqrt{2}F}[U_0\xi + \xi U_0^\dagger] - Z^{P3}\frac{i\Sigma}{2F^2}[U_0\xi^2 - \xi^2 U_0^\dagger]^{NSC} \\
&+\frac{i\Sigma}{12F^4}\bar{\Delta}(0)[U_0 - U_0^\dagger]\mathrm{Tr}[\xi^2]^{NSC} \\
&+\frac{\Sigma}{3\sqrt{2}F^3}[U_0\xi^3 + \xi^3 U_0^\dagger]^{NSC} + \frac{i\Sigma}{12F^4}[U_0\xi^4 - \xi^4 U_0^\dagger]^{NSC} \\
&-iL_4\frac{4\Sigma}{F^4}\left(\mathrm{Tr}[\partial_\mu\xi\partial^\mu\xi]^{NSC}\right)\times[U_0 - U_0^\dagger] - iL_5\frac{4\Sigma}{F^4}[U_0\partial_\mu\xi\partial^\mu\xi - \partial_\mu\xi\partial^\mu\xi U_0^\dagger]^{NSC} \\
&+\mathcal{O}(\epsilon^5), \qquad (32) \\
V^\mu(x) \;=\;& -\frac{FZ^{V1}}{\sqrt{2}}\left[U_0\partial^\mu\xi U_0^\dagger - \partial^\mu\xi\right] \\
&+\frac{iZ^{V2}}{2}\left[U_0(\partial^\mu\xi\xi - \xi\partial^\mu\xi)U_0^\dagger + (\partial^\mu\xi\xi - \xi\partial^\mu\xi)\right]^{NSC} \\
&+\frac{1}{3\sqrt{2}F}\left[U_0(\partial^\mu\xi\xi^2 - 2\xi\partial^\mu\xi\xi + \xi^2\partial^\mu\xi)U_0^\dagger - (\partial^\mu\xi\xi^2 - 2\xi\partial^\mu\xi\xi + \xi^2\partial^\mu\xi)\right]^{NSC} \\
&-\frac{i}{12F^2}\Big[U_0(\partial^\mu\xi\xi^3 - 3\xi\partial^\mu\xi\xi^2 + 3\xi^2\partial^\mu\xi\xi - \xi^3\partial^\mu\xi)U_0^\dagger \\
&\qquad\qquad +(\partial^\mu\xi\xi^3 - 3\xi\partial^\mu\xi\xi^2 + 3\xi^2\partial^\mu\xi\xi - \xi^3\partial^\mu\xi)\Big]^{NSC} \\
&-\frac{2iL_9}{F^2}\partial_\nu\left[U_0(\partial^\nu\xi\partial^\mu\xi - \partial^\mu\xi\partial^\nu\xi)U_0^\dagger + (\partial^\nu\xi\partial^\mu\xi - \partial^\mu\xi\partial^\nu\xi)\right]^{NSC} + \mathcal{O}(\epsilon^6), \qquad (33)
\end{aligned}
$$

where

$$
\begin{aligned}
Z^\Sigma \;&=\; 1 - \frac{N_f^2 - 1}{N_f F^2}\bar{\Delta}(0), && (34)\\
Z^\xi \;&=\; 1 - \frac{N_f}{6F^2}\bar{\Delta}(0), && (35)\\
Z^{P1} \;&=\; Z^\Sigma + \mathcal{O}(\epsilon^4), && (36)\\
Z^{P2} \;&=\; 1 - \frac{2N_f^2 - 3}{3N_f F^2}\bar{\Delta}(0), && (37)\\
Z^{P3} \;&=\; 1 - \frac{N_f}{2F^2}\bar{\Delta}(0) + \frac{1}{N_f F^2}\bar{\Delta}(0), && (38)\\
Z^{V1} \;&=\; 1 - \frac{2N_f}{3F^2}\bar{\Delta}(0), && (39)\\
Z^{V2} \;&=\; 1 - \frac{5N_f}{6F^2}\bar{\Delta}(0). && (40)
\end{aligned}
$$

In the above expression, the argument (x) of $\xi(x)$ is omitted for simplicity. In this work, we do not consider contact correlators at the same position, such as $\langle P(x)V^\mu(x)\rangle$. We have, therefore, only collected the terms linear in the sources $p(x)$ and $v_\mu(x)$.

Here we note that except for Z^{V2}, we can absorb all the Z factors into the redefinition

of the wave functions (ξ fields), or the coupling constants, by defining

$$\xi'(x) \equiv Z^{\xi}\xi(x), \tag{41}$$

$$\Sigma_{\rm eff} \equiv Z^{\Sigma}\Sigma, \tag{42}$$

$$F_{\rm eff} \equiv F\left(1 - \frac{N_f}{2F^2}\bar{\Delta}(0)\right). \tag{43}$$

Therefore, except for the 4-th term in Eq. (32), the vertex corrections of the two-point and three-point correlation functions can be obtained by simply replacing the coefficients of the LO results with the shifted ones $\Sigma_{\rm eff}$ and $F_{\rm eff}$, except for multiplying the coefficient of the second term in $V^{\mu}(x)$,

$$Z^{V2}/(Z^{\xi})^2 = 1 - \frac{N_f}{2F^2}\bar{\Delta}(0), \tag{44}$$

and the third term in $P(x)$,

$$Z^{P3'} \equiv \frac{Z^{P3}}{Z^{\Sigma}(Z^{\xi})^2}\left(\frac{F_{\rm eff}}{F}\right)^2 = 1 - \frac{N_f}{6F^2}\bar{\Delta}(0). \tag{45}$$

With this action, for any operator O (as a function of ξ and U_0) in the ϵ expansion,

$$O = O^{\rm LO} + O^{\rm NLO} + \cdots, \tag{46}$$

its expectation value is perturbatively evaluated as,

$$\begin{aligned}\langle O\rangle &\equiv \frac{\displaystyle\int \mathcal{D}U_0\mathcal{D}\xi\left[(O^{\rm LO}+O^{\rm NLO}+\cdots)e^{-\mathcal{S}^{\rm LO}-\mathcal{S}^{\rm NLO}+\cdots}\right]}{\displaystyle\int \mathcal{D}U_0\mathcal{D}\xi\left[e^{-\mathcal{S}^{\rm LO}-\mathcal{S}^{\rm NLO}+\cdots}\right]} \\ &= \langle\langle O^{\rm LO}\rangle_{\xi}\rangle_{U_0} + \left[\langle\langle O^{\rm NLO}\rangle_{\xi}\rangle_{U_0} - \langle\langle O^{\rm LO}\mathcal{S}^{\rm NLO}\rangle_{\xi}\rangle_{U_0} + \langle\langle O^{\rm LO}\rangle_{\xi}\rangle_{U_0}\langle\langle \mathcal{S}^{\rm NLO}\rangle_{\xi}\rangle_{U_0}\right] + \cdots,\end{aligned} \tag{47}$$

where we have used the following notations,

$$\langle O_1(U_0)\rangle_{U_0} \equiv \frac{\displaystyle\int \mathcal{D}U_0\, e^{\frac{\Sigma_{\rm eff}V}{2}{\rm Tr}[\mathcal{M}^{\dagger}U_0+U_0^{\dagger}\mathcal{M}]}\, O_1(U_0)}{\displaystyle\int \mathcal{D}U_0\, e^{\frac{\Sigma_{\rm eff}V}{2}{\rm Tr}[\mathcal{M}^{\dagger}U_0+U_0^{\dagger}\mathcal{M}]}}, \tag{48}$$

$$\langle O_2(\xi)\rangle_{\xi} \equiv \frac{\displaystyle\int \mathcal{D}\xi\, e^{-\int d^4x\frac{1}{2}{\rm Tr}[\xi(-\partial_{\mu}^2)\xi](x)}O_2(\xi)}{\displaystyle\int \mathcal{D}\xi\, e^{-\int d^4x\frac{1}{2}{\rm Tr}[\xi(-\partial_{\mu}^2)\xi](x)}}. \tag{49}$$

Note that, due to the use of NSC vertices, we do not need to calculate the fourth term in Eq. (47) since $\langle \mathcal{S}^{\rm NLO} \rangle_\xi = 0$.

In the usual $\theta = 0$ vacuum, $\mathcal{D}U_0$ denotes a Haar measure on $SU(N_f)$, while it should be replaced by $\mathcal{D}U_0 (\det U_0)^Q$ on $U(N_f)$, for a fixed topological sector as discussed in the previous subsection.

4. TWO-POINT FUNCTIONS

As we have mentioned in Sec. 2, the dominant finite volume effects on correlation functions comes from the pion's zero-momentum mode.

It is important that the zero-momentum mode itself does not depend on the space-time position x and always appears as an x-independent constant term or overall constants on x-dependent terms. Thus, it is not difficult to remove these zero-momentum mode's contribution from the correlation functions. In this section, we show an easiest example of these removals by taking the two-point pseudoscalar correlation functions.

4–a. LO calculation

Let us consider a pseudoscalar operator in the charged pion channel,

$$P^1(x) \equiv \frac{1}{2} \left([P(x)]_{12} + [P(x)]_{21} \right). \tag{50}$$

From the chiral symmetry, we can see that its two-point function satisfies

$$2\langle P^1(x) P^1(y) \rangle \;=\; \langle [P(x)]_{12} \, [P(x)]_{21} \rangle = \langle [P(x)]_{21} \, [P(x)]_{12} \rangle, \tag{51}$$

and

$$\langle [P(x)]_{12} [P(y)]_{12} \rangle \;=\; \langle [P(x)]_{21} [P(y)]_{21} \rangle = 0. \tag{52}$$

The quark field basis $[P(x)]_{ij}$ is convenient unless we consider the neutral sector of ChPT, since $\langle [P(x)]_{ij} \, [P(y)]_{ji} \rangle$ shares the same normalization of the so-called "connected" contribution of the conventional meson correlators in lattice QCD. Therefore, we use $[P(x)]_{ij}$ rather than the original $P^1(x)$ in the following analysis.

Now we show the two-point function result up to $\mathcal{O}(\epsilon^2)$,

$$\langle [P(x)]_{12}[P(y)]_{21}\rangle \;=\; -\frac{\Sigma_{\rm eff}^2}{4}\,\langle \mathcal{A}(U_0)\rangle_{U_0} + \frac{\Sigma_{\rm eff}^2}{2F_{\rm eff}^2 V}\,\langle \mathcal{B}(U_0)\rangle_{U_0} \sum_{p\neq 0}\frac{e^{ip(x-y)}}{p^2}, \tag{53}$$

where

$$\mathcal{A}(U_0) \;=\; [U_0 - U_0^\dagger]_{12}[U_0 - U_0^\dagger]_{21} + \frac{1}{2}([U_0 - U_0^\dagger]_{12})^2 + \frac{1}{2}([U_0 - U_0^\dagger]_{21})^2, \tag{54}$$

$$\mathcal{B}(U_0) \;=\; 2 + [U_0]_{11}[U_0]_{22} + [U_0^\dagger]_{11}[U_0^\dagger]_{22} - \Big([U_0]_{12} + [U_0^\dagger]_{12})([U_0]_{21} + [U_0^\dagger]_{21}\Big)/N_f. \tag{55}$$

Here $\Sigma_{\rm eff}$ or $F_{\rm eff}$ already includes some NLO contributions since we use the resummed Lagrangian with NSC vertices introduced in Sec. 3 3–c.

The result in Eq. (53) is a known in the literature, and one can evaluate $\langle \mathcal{A}(U_0)\rangle_{U_0}$ and $\langle \mathcal{B}(U_0)\rangle_{U_0}$ by a method shown in, for example, Ref. [19]. In particular, it is a special feature of the ϵ expansion that the x and y independent constant term appears, and we can use this feature for extracting Σ. In this study, however, this constant term which is the dominant finite volume effects, will be eliminated in the end of the calculation. Therefore, the second term of of Eq. (53) should be treated as the LO contribution in our calculation, and we need to calculate at one order higher.

4–b. NLO calculation

Next, we compute the NLO contribution. Since the contribution to the constant part will be eliminated at the end of our calculation, we simply neglect it here and in the following.

For the third term of Eq. (47), we obtain

$$\begin{aligned} -\langle\langle [P(x)]_{12}\,[P(y)]_{21}]^{\rm LO}\mathcal{S}^{\rm NLO}\rangle_\xi\rangle_{U_0} \;&=\; -\langle\langle [[P(x)]_{12}\,[P(y)]_{21}]^{\rm LO}\mathcal{S}_M^{\rm NLO}\rangle_\xi\rangle_{U_0} \\ &= \frac{\Sigma_{\rm eff}^2}{2F_{\rm eff}^2 V}\,\langle \mathcal{D}(U_0)\rangle_{U_0}\left(-M_{12}^2\right)\sum_{p\neq 0}\frac{e^{ip(x-y)}}{(p^2)^2}, \end{aligned} \tag{56}$$

with $M_{12}^2 \equiv (m_1+m_2)\Sigma_{\rm eff}/F^2$, and the dimensionless U_0 integral part is given by

$$\mathcal{D}(U_0) \;=\; \sum_{k=0}^{4} \mathcal{D}^k(U_0), \tag{57}$$

$$\mathcal{D}^0(U_0) \;=\; [U_0]_{11} + [U_0]_{22} + [U_0^\dagger]_{11} + [U_0^\dagger]_{22}, \tag{58}$$

$$\mathcal{D}^1(U_0) \;=\; \frac{N_f}{\mu_1+\mu_2}(2 - [U_0]_{11}[U_0]_{22} - [U_0^\dagger]_{11}[U_0^\dagger]_{22}), \tag{59}$$

$$\mathcal{D}^2(U_0) \;=\; \sum_{i,j} \frac{\delta_{i1}\delta_{2j}+\delta_{i2}\delta_{1j}}{2} \left[[U_0]_{ii} \left(\frac{[U_0\mathcal{M}^\dagger U_0]_{jj} - m_j}{m_1+m_2} + \frac{2N_f}{\mu_1+\mu_2}[U_0]_{jj} \right) + h.c. \right], \tag{60}$$

$$\begin{aligned} \mathcal{D}^3(U_0) \;=\; & -\sum_{i,j} \frac{\delta_{i1}\delta_{2j}+\delta_{i2}\delta_{1j}}{N_f} \left([U_0]_{ij} + [U_0^\dagger]_{ij} \right) \\ & \times \left[\frac{[U_0\mathcal{M}^\dagger U_0]_{ji} + [U_0^\dagger \mathcal{M} U_0^\dagger]_{ji}}{m_1+m_2} + \frac{N_f}{\mu_1+\mu_2} \left([U_0]_{ji} + [U_0^\dagger]_{ji} \right) \right], \end{aligned} \tag{61}$$

$$\mathcal{D}^4(U_0) \;=\; \frac{\left([U_0]_{12} + [U_0^\dagger]_{12} \right) \left([U_0]_{21} + [U_0^\dagger]_{21} \right)}{N_f} \left(\frac{1}{N_f} \sum_i^{N_f} \frac{m_i \left([U_0]_{ii} + [U_0^\dagger]_{ii} \right)}{m_1+m_2} + \frac{N_f}{\mu_1+\mu_2} \right), \tag{62}$$

with $\mu_i = m_i \Sigma_{\rm eff} V$. Here we have shown the result with non-degenerate N_f–flavor quark masses m_i's, which is the more general set-up than that of in this work. The result with degenerate masses can be obtained by simply setting as $m_i \to m$ in the above formulas. Note that we have neglected trivially vanishing U_0 integrals like $\langle [U_0]_{ij} \rangle_{U_0} = 0$ for $i \neq j$.

The second term of Eq. (47) is given by

$$\langle \langle [[P(x)]_{12} [P(y)]_{21}]^{\rm NLO} \rangle_\xi \rangle_{U_0} \;=\; -\frac{\Sigma_{\rm eff}^2}{4F_{\rm eff}^4 V^2} \langle \mathcal{C}(U_0) \rangle_{U_0} \sum_{p_1 \neq 0} \sum_{p_2 \neq 0} \frac{e^{ip_1(x-y)}}{p_1^2} \frac{e^{ip_2(x-y)}}{p_2^2}, \tag{63}$$

where

$$\begin{aligned} \mathcal{C}(U_0) \;=\; & \left(\frac{4}{N_f} - N_f \right) \left(2 - [U_0]_{11}[U_0]_{22} - [U_0^\dagger]_{11}[U_0^\dagger]_{22} \right) \\ & + \left(1 + \frac{2}{N_f^2} \right) \left([U_0]_{12} - [U_0^\dagger]_{12} \right) \left([U_0]_{21} - [U_0^\dagger]_{21} \right). \end{aligned} \tag{64}$$

To summarize our results above, we define the "massive" propagator,

$$\bar{\Delta}(x; M^2) \;\equiv\; \frac{1}{V} \sum_{p \neq 0} \frac{e^{ipx}}{p^2 + M^2}, \tag{65}$$

and using the relation,

$$\frac{1}{p^2} - M^2 \frac{1}{(p^2)^2} = \frac{1}{p^2+M^2} + \mathcal{O}(M^4), \tag{66}$$

for $M \sim \mathcal{O}(\epsilon^2)$, the correlator can be written in a simple form as

$$\langle [P(x)]_{12} [P(y)]_{21} \rangle \;=\; const. + \frac{\Sigma_{\rm eff}^2}{2F_{\rm eff}^2 V} \langle \mathcal{B}(U_0) \rangle_{U_0} \sum_{p \neq 0} \frac{e^{ip(x-y)}}{p^2 + M_{12}^2 Z_M^{\rm 2pt}} - \frac{\Sigma_{\rm eff}^2}{4F_{\rm eff}^4 V^2} \langle \mathcal{C}(U_0) \rangle_{U_0} \sum_{p_1 \neq 0} \sum_{p_2 \neq 0} \frac{e^{ip_1(x-y)}}{p_1^2} \frac{e^{ip_2(x-y)}}{p_2^2}, \quad (67)$$

where *const.* represents the constant term which will be eliminated below, and

$$Z_M^{\rm 2pt} \;=\; 1 + \frac{\langle \mathcal{D}(U_0) - \mathcal{B}(U_0) \rangle_{U_0}}{\langle \mathcal{B}(U_0) \rangle_{U_0}}. \quad (68)$$

The above result Eq. (67) is not completely new but have already derived for the degenerate case by Hansen [16] (with the explicit form for the constant term, which depends on the NLO LEC L_i's). The only difference here comes from the resummation of the *mass* effect using Eq. (65). Although this resummation should cause no essential numerical difference from the original form, the form after performing an integration over x in the spatial direction looks quite different : the resummation gives a formula with cosh function, while the original non-resummed one gives a polynomial.

In the literature, the polynomials in the correlators are often mentioned as a special feature of the ϵ expansion. However, this is not absolutely true. Let us consider an exactly massless quark theory. Even in this theory, the ξ fields have a finite mass $\sqrt{N_f/F^2V}$ which comes from the measure term (See Eq. (31)), and this theory describes a hybrid system of *massive* ξ fields and completely random field U_0 (having no action). In this extreme case, the propagation of the ξ fields has a form of exponential decay, and the polynomial form in the ϵ expansion is just an approximation of it. The mass resummation Eq. (65) achieves a smooth connection to the p expansion[1], which is important in another special limit $m\Sigma V \to \infty$ with keeping $M_\pi L < 1$, where the both of ϵ and p expansions are available. More specifically, the p regime result can be easily reproduced from the ϵ regime result Eq. (67) by taking the $V \to \infty$ limit which gives $\langle \mathcal{B}(U_0) \rangle_{U_0} \to 4$, $\langle \mathcal{A}(U_0) \rangle_{U_0} = \langle \mathcal{C}(U_0) \rangle_{U_0} \to 0$, and $Z_M^{\rm 2pt} \to 1$. For these reasons, it is expected that this resummation Eq. (65) gives a better convergence in the ϵ expansion as well as a practical advantage of equally treating the zero and non-zero momentum modes.

[1]For more rigorous arguments, see Refs. [20, 33].

The third term of Eq. (67) is peculiar one in the ϵ regime, which originally comes from a 3-pion state, consisting of two having non-zero momenta and one having zero momentum. Up to this order, it looks a propagation of massless particles. However, for the same reason discussed above, these propagators should also have masses which comes from higher order corrections, at least, the one from the measure term in Eq. (18). We expect that propagations like this multi particle state cannot reach a long-distance, compared to the single particle propagation. In the following analysis, thus, we simply drop this NLO term and similar terms in the three-point functions. Of course, we cannot justify this dropping the terms in the ϵ expansion of ChPT, since the expansion in the dimensionful parameters does not know how small the dimensionless quantity is. This truncation may be numerically justified by checking the plateau of the effective mass in lattice QCD simulations [14].

4–c. Removing dominant finite volume effects in the ϵ expansion

We are ready to cancel the dominant finite volume effects which comes from the zero-modes contribution. First, we consider an insertion of spatial momentum to the operators. Namely, we define

$$\begin{aligned} C_{PP}^{\rm 2pt}(t;\mathbf{p}) &\equiv \langle [P(x_0;\mathbf{p})]_{12}[P(y_0;-\mathbf{p})]_{21}\rangle\,, \\ [P(x_0;\mathbf{p})]_{ij} &\equiv \int d^3x\, e^{-i\mathbf{p}\cdot\mathbf{x}}[P(x)]_{ij}, \end{aligned} \tag{69}$$

where x_0 and y_0 is the temporal element of x and y, respectively, $t = x_0 - y_0$, and $\mathbf{p} = 2\pi(n_x, n_y, n_z)/L$ is the spatial momentum. Then, the unwanted constant part *const.* automatically vanish for $\mathbf{p} \neq \mathbf{0}$. This should be intuitively recognized, since the higher energy states having momenta are less sensitive to the finite volume. Even in the case $\mathbf{p} = \mathbf{0}$, we can eliminate the constant part by a simple subtraction with respect to time: $\Delta_t[P(t;\mathbf{p})]_{ij} \equiv [P(t;\mathbf{p})]_{ij} - [P(t_{\rm ref};\mathbf{p})]_{ij}$ where $t_{\rm ref}$ is a reference time-slice.

Second, we take a ratio of the correlators wih different momenta. For example, by setting as $y_0 = 0$ and $x_0 = t$, we have

$$\begin{aligned} R^{\rm 2pt}(t;\mathbf{p}) &\equiv \frac{\langle [P(t;\mathbf{p})]_{12}[P(0;-\mathbf{p})]_{21}\rangle}{\langle \Delta_t[P(t;\mathbf{0})]_{12}[P(0;\mathbf{0})]_{21}\rangle} \\ &= \frac{E^{\rm 2pt}(\mathbf{0})\sinh\left(E^{\rm 2pt}(\mathbf{0})T/2\right)}{E^{\rm 2pt}(\mathbf{p})\sinh\left(E^{\rm 2pt}(\mathbf{p})T/2\right)} \times \frac{\cosh(E^{\rm 2pt}(\mathbf{p})(t-T/2))}{\cosh(E^{\rm 2pt}(\mathbf{0})(t-T/2)) - \cosh(E^{\rm 2pt}(\mathbf{0})(t_{\rm ref}-T/2))}, \end{aligned} \tag{70}$$

where

$$E^{\rm 2pt}(\mathbf{p}) \equiv \sqrt{M_{12}^2 Z_M^{\rm 2pt} + \mathbf{p}^2}. \tag{71}$$

The ratio $R^{\rm 2pt}(t;\mathbf{p})$ does not depend on $\langle\mathcal{A}(U_0)\rangle_{U_0}$ or $\langle\mathcal{B}(U_0)\rangle_{U_0}$ anymore. This expression is exactly same as the same ratio in the p expansion, except the mass correction factor $Z_M^{\rm 2pt}$. Namely, the features of the ϵ regime in the two-point correlator have been minimized. It is also important that $R^{\rm 2pt}(t;\mathbf{p})$ is finite even in the $E^{\rm 2pt}(\mathbf{0}) \to 0$ limit.

Since the above ratio $R^{\rm 2pt}(t;\mathbf{p})$ does not depend on LEC's of ChPT, it is not phenomenologically interesting. However, it provides a good test for lattice QCD to check the validity of the above arguments. JLQCD collaboration [14] checked the difference between the ratio $R^{\rm 2pt}(t;\mathbf{p})$ and the numerical data in the both cases with $M_{12}\sqrt{Z_M^{\rm 2pt}} = 0$ and 100 MeV, and found a fairly good agreement. This means that the NLO corrections in $\sqrt{Z_M^{\rm 2pt}}$ and the third term of Eq. (67) we have neglected are actually small.

Since the facts that the pion's zero-momentum mode is the x-independent and gives the dominant finite volume effects are universal and true in any correlation functions at any sizes of the volume, our method is expected to have wide applications. Namely, by inserting momenta to the correlators and taking ratios of them, we can generally construct a less sensitive quantity to the volume than the original ones. We will see this argument is true for the three-point functions in the next section.

5. THREE-POINT FUNCTION

In this section, we calculate the pseudoscalar-vector-pseudoscalar three-point function in a finite volume in the ϵ expansion of ChPT, from which the vector pion form factor can be extracted. However, the pion form factor itself is not described within ChPT alone. In numerical studies [27, 28] show that the results include large contribution from the vector meson, which cannot be explained by ChPT. Even in such a case, since the propagations of the heavier hadrons, including the vector mesons, do not reach far away, we still expect to be able to treat the correction from the finite volume effects within ChPT. Thus, in this section, we calculate the three-point functions and the finite volume effects on it within the ϵ expansion of ChPT.

5–a. Three-point functions and form factors

First, we briefly review a relation between the three-point functions and the pion form factors. The vector form factor F_V is defined by

$$\langle \pi^a(p_2)|V_\mu^b(x)|\pi^c(p_1)\rangle \;=\; i\epsilon^{abc}(p_1+p_2)_\mu F_V(t), \tag{72}$$

where $|\pi^a(p)\rangle$ denotes the on-shell pion state with momentum p and $t=(p_1-p_2)^2$ is the momentum transfer. $V_\mu^b(x)$ is the coefficient of an $SU(2)$ generator τ^b in the vector operator.

For lattice QCD calculations, to take $b=3$ component is convenient:

$$V_\mu^3(x) \;=\; \frac{1}{2}\bar{u}\gamma_\mu u(x) - \frac{1}{2}\bar{d}\gamma_\mu d(x). \tag{73}$$

Using a conventional notation

$$|\pi^1(p)\rangle \;=\; \frac{|\pi^+(p)\rangle + |\pi^-(p)\rangle}{\sqrt{2}}, \quad |\pi^2(p)\rangle = \frac{|\pi^+(p)\rangle - |\pi^-(p)\rangle}{\sqrt{2}i}, \tag{74}$$

with $|\pi^\pm(p)\rangle$ denotes the charged pion state, and iso-spin symmetry (with assuming $m_u = m_d = m$),

$$\langle \pi^+(p_2)|V_\mu^3(x)|\pi^+(p_1)\rangle \;=\; -\langle \pi^-(p_2)|V_\mu^3(x)|\pi^-(p_1)\rangle, \tag{75}$$

as well as the electric charge conservation,

$$\langle \pi^+(p_2)|V_\mu^3(x)|\pi^-(p_1)\rangle \;=\; \langle \pi^-(p_2)|V_\mu^3(x)|\pi^+(p_1)\rangle = 0, \tag{76}$$

one can obtain a simpler formula,

$$\langle \pi^+(p_2)|V_\mu^3(x)|\pi^+(p_1)\rangle \;=\; (p_1+p_2)_\mu F_V(t). \tag{77}$$

For the isospin zero current,

$$V_\mu^0(x) \;=\; \bar{u}\gamma_\mu u(x) + \bar{d}\gamma_\mu d(x), \tag{78}$$

it is also important to note that its form factor is zero:

$$\langle \pi^a(p_2)|V_\mu^0(x)|\pi^b(p_1)\rangle = 0 \quad \text{for any } a,b, \tag{79}$$

since the Baryon charge of the pions is zero. In ChPT, this situation is more directly shown by $V_\mu^0(x) = \mathrm{Tr}\, V_\mu(x) = 0$ in Eq. (33). Namely, there exists no corresponding current within ChPT. Therefore, for the electro-magnetic current,

$$J_\mu^{EM} \;\equiv\; V_\mu^3(x) + \frac{1}{6}V_\mu^0(x) = \frac{2}{3}\bar{u}\gamma_\mu u(x) - \frac{1}{3}\bar{d}\gamma_\mu d(x), \tag{80}$$

one can show an identity,

$$\langle\pi^+(p_2)|V_\mu^3(x)|\pi^+(p_1)\rangle \;=\; \langle\pi^+(p_2)|J_\mu^{EM}(x)|\pi^+(p_1)\rangle. \tag{81}$$

Namely, for the pions, it is not necessary to distinguish the vector form factor from the electro-magnetic form factor.

In the literature, a calculation of the finite volume effects on the hadronic matrix elements is often performed by replacing the quantum loop momentum integrations by a discrete momentum summation. In such a calculation, it is implied that one can still apply the same LSZ reduction formula in the $V \to \infty$ limit, to relate the form factor to the three-point function,

$$\begin{aligned}\int d^4x e^{ip_2x} \int d^4z e^{-ip_1z} \langle [P(x)]_{12}\, V_\mu^3(y)\, [P(z)]_{21}\rangle \\ = \frac{\langle 0|\,[P(0)]_{12}\,|\pi^+(p_2)\rangle\langle\pi^+(p_1)|\,[P(0)]_{21}\,|0\rangle}{(p_1^2+m_\pi^2)(p_2^2+m_\pi^2)} \langle\pi^+(p_2)|V_\mu^3(y)|\pi^+(p_1)\rangle.\end{aligned} \tag{82}$$

However, in a finite volume, this relation is non-trivial, and finite volume correction to the reduction formula itself should be considered. In this work, we study the finite volume correction within ChPT to

$$\langle [P(x)]_{12}\, [V_\mu(y)]_{ii}\, [P(z)]_{21}\rangle, \tag{83}$$

with a general flavor index i. We will soon see that $\langle [P(x)]_{12}\, [V_\mu(y)]_{ii}\, [P(z)]_{21}\rangle = (\delta_{i1} - \delta_{i2})\langle [P(x)]_{12}\, V_\mu^3(y)\, [P(z)]_{21}\rangle$. We then perform its Fourier transformation with non-zero momenta, and show how to disentangle the pion form factor from the correlators.

5–b. LO contribution

In the following, we assume $t = x_0 - y_0 > 0$, $t' = y_0 - z_0 > 0$. And further, we also assume t, t', $t + t' < T/2$ to suppress the effect which comes from modes wrapping around our periodic lattice.

The LO contribution to the three-point function can be easily computed in the same way

as the two-point function above,

$$\langle [P(x)]_{12} [V_\mu(y)]_{ii} [P(z)]_{21} \rangle = (\delta_{i2} - \delta_{i1}) \left(\frac{Z^{V2}}{(Z^\xi)^2} \right) \frac{i\Sigma_{\rm eff}^2}{4F_{\rm eff}^2 V^2} \langle \mathcal{E}(U_0) \rangle_{U_0} \times \sum_{p_1 \neq 0} \sum_{p_2 \neq 0} \frac{-ip_1^\mu - ip_2^\mu}{p_1^2 p_2^2} e^{ip_1(x-y)} e^{ip_2(y-z)}, \tag{84}$$

where

$$\mathcal{E}(U_0) = \Big(2 + 2[U_0]_{11}[U_0]_{22} + 2[U_0^\dagger]_{11}[U_0^\dagger]_{22} + [U_0]_{11}[U_0^\dagger]_{11} + [U_0]_{22}[U_0^\dagger]_{22} - [U_0]_{12}[U_0^\dagger]_{21} - [U_0]_{21}[U_0^\dagger]_{12} \Big). \tag{85}$$

Here, we have just neglected the t and t' independent terms since they will automatically cancel in the end of our calculation.

We have also neglected contributions from ξ's connected in unusual orders, like x–z–y or z–x–y, including the long propagation between x and z, which is expected to be exponentially suppressed. This expectation is not correct for the zero-momentum contribution at LO. However, as we have mentioned in the previous section, we can expect that the NLO corrections give a "mass" to the correlators and long-range correlation is suppressed compared to the main result. One can numerically check this expectation by looking whether unexpected $|x - z|$ dependence is detected or not.

5–c. NLO contribution

Next, we calculate the NLO corrections to the three-point function. As we saw in the two-point function, the contribution from $\mathcal{S}_M^{\rm NLO}$ can be absorbed to the mass as corrections: together with the LO contribution, one can obtain

$$\langle \langle [P(x)]_{12} [V_\mu(y)]_{ii} [P(z)]_{21}]^{\rm LO} (1 - \mathcal{S}_M^{\rm NLO}) \rangle_\xi \rangle_{U_0} = (\delta_{i2} - \delta_{i1}) \frac{i\Sigma_{\rm eff}^2}{4F_{\rm eff}^2 V^2} \langle \mathcal{E}(U_0) \rangle_{U_0} \sum_{p_1 \neq 0} \sum_{p_2 \neq 0} \frac{-ip_1^\mu - ip_2^\mu}{(p_1^2 + M_{12}^2 Z_M^{\rm 3pt})(p_2^2 + M_{12}^2 Z_M^{\rm 3pt})} e^{ip_1(x-y)} e^{ip_2(y-z)}, \tag{86}$$

where

$$Z_M^{\rm 3pt} = 1 + \frac{N_f}{M_{12}^2 F^2 V} + \frac{\langle \mathcal{G}(U_0) + \mathcal{H}(U_0) \rangle_{U_0}}{\langle \mathcal{E}(U_0) \rangle_{U_0}}, \tag{87}$$

$$
\begin{aligned}
\mathcal{G}(U_0) \equiv \frac{1}{4}\Big[\Big\{&([U_0]_{22}+[U_0^\dagger]_{22}-2)(2+[U_0]_{11}[U_0]_{22}+[U_0^\dagger]_{11}[U_0^\dagger]_{22})\\
&+8([U_0]_{22}+[U_0^\dagger]_{22})\\
&-6[U_0]_{11}[U_0]_{22}-6[U_0^\dagger]_{11}[U_0^\dagger]_{22}-4[U_0]_{22}[U_0^\dagger]_{22}\\
&-([U_0]_{22}+[U_0^\dagger]_{22}-4)([U_0]_{12}[U_0^\dagger]_{21}+[U_0^\dagger]_{12}[U_0]_{21})\\
&-([U_0]_{12}[U_0]_{21}[U_0]_{22}+[U_0^\dagger]_{12}[U_0^\dagger]_{21}[U_0^\dagger]_{22})\\
&+2([U_0]_{11}+[U_0^\dagger]_{11}-2)(1+[U_0]_{22}[U_0^\dagger]_{22})\Big\}\\
&+([U_0]_{11}+[U_0^\dagger]_{22})([U_0\mathcal{M}^\dagger U_0]_{22}/m-1)\\
&+([U_0^\dagger]_{11}+[U_0]_{22})([U_0^\dagger\mathcal{M}U_0^\dagger]_{22}/m-1)\\
&+2[U_0]_{22}([U_0\mathcal{M}^\dagger U_0]_{11}/m-1)+2[U_0^\dagger]_{22}([U_0^\dagger\mathcal{M}U_0^\dagger]_{11}/m-1)\\
&-([U_0]_{12}[U_0^\dagger]_{21}[U_0^\dagger]_{22}+[U_0^\dagger]_{12}[U_0]_{21}[U_0]_{22})\\
&-([U_0^\dagger]_{21}[U_0\mathcal{M}^\dagger U_0]_{12}/m+[U_0]_{21}[U_0^\dagger\mathcal{M}U_0^\dagger]_{12}/m)\Big],
\end{aligned}
\tag{88}
$$

$$
\mathcal{H}(U_0) \equiv -\frac{1}{2N_f}\Big[([U_0]_{12}+[U_0^\dagger]_{12})([U_0\mathcal{M}^\dagger U_0]_{21}/m+[U_0^\dagger\mathcal{M}U_0^\dagger]_{21}/m)\Big]. \tag{89}
$$

For the operator, we have a correction from the L_9 term:

$$
\begin{aligned}
\langle\langle[[P(x)]_{12}\,[V_\mu(y)]_{ii}\,[P(x)]_{21}]^{L_9}\rangle_\xi\rangle_{U_0} \;=\;&\\
&(\delta_{i2}-\delta_{i1})\frac{i\Sigma_{\rm eff}^2}{4F_{\rm eff}^2V^2}\,\langle\mathcal{E}(U_0)\rangle_{U_0}\left(-\frac{2L_9}{F_{\rm eff}^2}\right)\\
&\times\sum_{p_1\neq0}\sum_{p_2\neq0}\frac{i\,[p_2\cdot(p_1-p_2)]\,(p_1)_\mu-i\,[p_1\cdot(p_1-p_2)]\,(p_2)_\mu}{p_1^2\,p_2^2}e^{ip_1(x-y)}e^{ip_2(y-z)}.
\end{aligned}
\tag{90}
$$

The correction from $\mathcal{S}_K^{\rm NLO}$ term is written as

$$
\begin{aligned}
-\langle\langle[P(x)]_{12}\,[V_\mu(y)]_{ii}\,[P(z)]_{21}]^{\rm LO}\mathcal{S}_K^{\rm NLO}\rangle_\xi\rangle_{U_0} \;=\;&\\
&(\delta_{i2}-\delta_{i1})\frac{i\Sigma_{\rm eff}^2}{4F_{\rm eff}^2V^2}\,\langle\mathcal{E}(U_0)\rangle_{U_0}\\
&\times\left(-\frac{N_f}{2F_{\rm eff}^2}\right)\sum_{p_1\neq0}\sum_{p_2\neq0}\frac{-i(p_1+p_2)^\nu I_{\mu\nu}(-p_1^0+p_2^0,-\mathbf{p}_1+\mathbf{p}_2)}{p_1^2\,p_2^2}e^{ip_1(x-y)}e^{ip_2(y-z)},
\end{aligned}
\tag{91}
$$

where

$$
I_{\mu\nu}(q_0,\mathbf{q}) \equiv \frac{1}{V}\sum_{p\neq0,q}\frac{p^\mu(q^\nu-2p^\nu)}{p^2(q-p)^2}\quad(q^2=q_0^2+\mathbf{q}^2). \tag{92}
$$

We summarize all the above results for the $\mu = 0$ case, inserting momenta $\mathbf{p}_f$ and $\mathbf{p}_i$. Using the notations $E^{3\mathrm{pt}}(\mathbf{p}) \equiv \sqrt{M_{12}^2 Z_M^{3\mathrm{pt}} + \mathbf{p}^2}$, and

$$c(\mathbf{p},t) \;=\; \frac{\cosh[E^{3\mathrm{pt}}(\mathbf{p})(t-T/2)]}{2E^{3\mathrm{pt}}(\mathbf{p})\sinh[E^{3\mathrm{pt}}(\mathbf{p})T/2]}, \qquad s(\mathbf{p},t) = \frac{\sinh[E^{3\mathrm{pt}}(\mathbf{p})(t-T/2)]}{2E^{3\mathrm{pt}}(\mathbf{p})\sinh[E^{3\mathrm{pt}}(\mathbf{p})T/2]}, \tag{93}$$

one can express the result as

$$\begin{aligned} C^{PV_0P}(t,t';\mathbf{p}_f,\mathbf{p}_i) \;&\equiv\; \langle [P(x_0,-\mathbf{p}_f)]_{12}\, V_0^3(y_0,\mathbf{q})\, [P(z_0,\mathbf{p}_i)]_{21}\rangle \\ &=\; -\frac{L^3\Sigma_{\mathrm{eff}}^2}{4F_{\mathrm{eff}}^2}\,\langle \mathcal{E}(U_0)\rangle_{U_0}\,\delta^{(3)}_{\mathbf{q},\mathbf{p}_f-\mathbf{p}_i} Z_k F_V(q_0,\mathbf{q}) \\ &\quad\times \left[iE^{3\mathrm{pt}}(\mathbf{p}_i)c(\mathbf{p}_f,t)s(\mathbf{p}_i,t') + iE^{3\mathrm{pt}}(\mathbf{p}_f)s(\mathbf{p}_f,t)c(\mathbf{p}_i,t')\right]. \end{aligned} \tag{94}$$

Here, as mentioned in the above, we have omitted the two-pion-like propagations, and the long-distance correlators depend on $x_0 - z_0 = t + t'$, since they are expected to be exponentially small.

The vector form factor $F_V(q_0,\mathbf{q})$ is obtained as

$$F_V(q_0,\mathbf{q}) \;=\; \frac{Z^{V2}}{(Z^\xi)^2} - \frac{2L_9}{F_{\mathrm{eff}}^2}q^2 - \frac{N_f}{2F_{\mathrm{eff}}^2}\left(l(q_0,\mathbf{q}) - l_{00}\right), \tag{95}$$

where $l(q_0,\mathbf{q})$ is a part of $I_{0\nu}(q_0,\mathbf{q})$ which is proportional to $\delta_{0\nu}$. We don't have to include another part proportional to $q_0 q_\nu$ since it is contracted with a perpendicular vector $\bar{q}^\nu$ to q_μ. Namely, $l(q_0,\mathbf{q})$ is given by

$$l(q_0,\mathbf{q}) \;=\; I_{0\nu}(q_0,\mathbf{q})\bar{q}^\nu/\bar{q}_0. \tag{96}$$

More details are shown in Appendix B.

Note in the above formula, the (finite) renormalization factor

$$Z_k \;=\; 1 - \frac{N_f}{2F_{\mathrm{eff}}^2}l_{00}, \qquad l_{00} \equiv -\frac{1}{4\pi^2}\sum_{b\neq 0}\frac{1}{|b_\mu|^2}\left(1 - \frac{2(b_0)^2}{|b_\mu|^2}\right), \tag{97}$$

where the summation is taken over the vector $b_\mu = (n_0 T, n_1 L, n_2 L, n_3 L)$, is introduced so that $F_V(0,\mathbf{0}) = 1$ is maintained even in a finite volume. Therefore, only the finite volume effects come from the non-zero modes are contained in $F_V(q_0,\mathbf{q})$. This remaining finite volume effects are expected to be perturbatively small, and we will discuss the details of this in the next section.

Finally, let us discuss the renormalization of the above formula Eq. (95). Since the finite volume effects are free from UV divergences, to consider the $V \to \infty$ limit of $F_V(q_0,\mathbf{q})$ is

sufficient. The quadratic divergence in $Z^{V2}/(Z^{\xi})^2$ precisely cancels with that in $l(q_0, \mathbf{q})$. Therefore, we only need a renormalization of the logarithmic divergence of $l(q_0, \mathbf{q})$ by the re-definition of L_9.

Employing the dimensional regularization, we can evaluate its logarithmic divergence as

$$\begin{aligned}\lim_{V\to\infty} l(q_0, \mathbf{q}) &= \frac{\bar{q}^{\nu}}{\bar{q}_0} \int \frac{d^d p}{(2\pi)^d} \frac{-2p_0 p_{\nu}}{p^2 (p-q)^2} \\ &= \frac{1}{16\pi^2} \left\{ \frac{q^2}{6} \left(\frac{2}{\epsilon} + 1 - \gamma_E + \ln 4\pi - \ln \mu_{sub}^2 \right) - \frac{q^2}{6} \ln \frac{q^2}{\mu_{sub}^2} + \frac{5}{18} q^2 \right\}, \quad (98)\end{aligned}$$

where $\epsilon = 4 - d$, $\gamma_E = 0.57721\cdots$ is the Euler's constant, and μ_{sub} denotes the subtraction scale. This divergence can be absorbed in the renormalization of L_9:

$$L_9^r(\mu_{sub}) \equiv L_9 - \frac{N_f}{12} \times \frac{1}{16\pi^2} \left(-\frac{1}{\epsilon} - \frac{1}{2}(-\gamma_E + \ln 4\pi + 1 - \ln \mu_{sub}^2) \right), \quad (99)$$

and one obetains the vector form factor in the infinite volume limit,

$$F_V^{\infty}(q_0, \mathbf{q}) = 1 - \frac{2L_9^r(\mu_{sub})}{F_{\rm eff}^2} q^2 - \frac{N_f}{2F_{\rm eff}^2} \frac{1}{16\pi^2} \left[-\frac{1}{6} q^2 \ln \frac{q^2}{\mu_{sub}^2} + \frac{5}{18} q^2 \right], \quad (100)$$

which agrees with the known (massless limit of) result within ChPT. Lattice and experimental results for this are, for example, $10^3 \times L_9^r = 3.08(23)(51)$[35], and $5.93(43)$[34], respectively (we do not need these values for the following analysis). We should note that $F_V^{\infty}(q_0, \mathbf{q})$ cannot be expected to describe the lattice data well, since the physics beyond ChPT is omitted in our calculation within the ChPT. Nevertheless, we can still expect that the finite volume correction: $F_V(q_0, \mathbf{q}) - F_V^{\infty}(q_0, \mathbf{q})$ is well described within ChPT, which will be discussed in the next section.

6. EXTRACTION OF THE VECTOR FORM FACTOR OF PION

In this section, we explain how to eliminate the leading contribution of the zero-momentum pion mode from the correlator, and how to extract the vector form factor of the pions. Although, there still exists finite volume effects from non-zero momentum modes' contribution, they are sub-leading one expected to be small. We perform the one-loop calculation of the non-zero momentum modes, and numerical estimation which shows that this remaining finite volume effects are actually a small perturbation.

6–a. Removing dominant finite volume effects from the pion zero mode

In the previous section, the t–independent or t'–independent terms have been neglected. In the final form Eq. (94), if both of $\mathbf{p}_i$ and $\mathbf{p}_f$ are non-zero, these neglected terms are actually dropped automatically. However, even if these momenta are zero, we can also eliminate them by taking subtraction of the correlators at different time-slices, $\Delta_t f(t) \equiv f(t) - f(t_{\rm ref})$, $\Delta_{t'} f(t') \equiv f(t') - f(t'_{\rm ref})$, with $t_{\rm ref}$ and $t'_{\rm ref}$, respectively. We used similar procedure in the two-point correlators.

To suppress the contribution of pion modes wrapping around our periodic lattice, we should take $t_{\rm ref} + t'_{\rm ref} < T/2$, and then, $t_{\rm ref} = t'_{\rm ref} \sim T/4$ would be optimal. In the following, we set as $t'_{\rm ref} = t_{\rm ref}$, for simplicity.

Noting the above time-slice subtraction and $F_V(0,\mathbf{0}) = 1$, it is useful for extracting the vector pion form factor to define the ratios as

$$\begin{aligned} R_1(t,t';\mathbf{p}_f,\mathbf{p}_i) &\equiv \frac{C^{PV_0P}(t,t';\mathbf{p}_f,\mathbf{p}_i)}{\Delta_t\Delta_{t'}C^{PV_0P}(t,t';\mathbf{0},\mathbf{0})} \\ &= F_V(q_0,\mathbf{q}) \times \frac{E^{\rm 3pt}(\mathbf{p}_i)c(\mathbf{p}_f,t)s(\mathbf{p}_i,t') + E^{\rm 3pt}(\mathbf{p}_f)s(\mathbf{p}_f,t)c(\mathbf{p}_i,t')}{E^{\rm 3pt}(\mathbf{0})\Delta_t c(\mathbf{0},t)\Delta_{t'}s(\mathbf{0},t') + E^{\rm 3pt}(\mathbf{0})\Delta_t s(\mathbf{0},t)\Delta_{t'}c(\mathbf{0},t')}, \\ R_2(t,t';\mathbf{0},\mathbf{p}_i) &\equiv \frac{\Delta_t C^{PV_0P}(t,t';\mathbf{0},\mathbf{p}_i)}{\Delta_t\Delta_{t'}C^{PV_0P}(t,t';\mathbf{0},\mathbf{0})} \\ &= F_V(q_0,\mathbf{q}) \times \frac{E^{\rm 3pt}(\mathbf{p}_i)\Delta_t c(\mathbf{0},t)s(\mathbf{p}_i,t') + E^{\rm 3pt}(\mathbf{0})\Delta_t s(\mathbf{0},t)c(\mathbf{p}_i,t')}{E^{\rm 3pt}(\mathbf{0})\Delta_t c(\mathbf{0},t)\Delta_{t'}s(\mathbf{0},t') + E^{\rm 3pt}(\mathbf{0})\Delta_t s(\mathbf{0},t)\Delta_{t'}c(\mathbf{0},t')}. \end{aligned} \tag{101}$$

It is important that we can determine the t and t' dependences uniquely once $M_{12}\sqrt{Z_M^{\rm 3pt}}$ is given. Therefore, one can extract $F_V(q_0,\mathbf{q})$ by performing a one-parameter fit, taking $M_{12}\sqrt{Z_M^{\rm 3pt}}$ as a free parameter.

In the numerical lattice analysis, one could also try taking further ratios with two-point

functions. Namely,

$$
\begin{aligned}
R_1'(t,t';\mathbf{p}_f,\mathbf{p}_i) \;\equiv\; & \frac{C^{PV_0P}(t,t';\mathbf{p}_f,\mathbf{p}_i)}{\Delta_t\Delta_{t'}C^{PV_0P}(t,t';\mathbf{0},\mathbf{0})} \\
& \times\left(\frac{-\Delta_t C^{2\mathrm{pt}}_{PP}(t,\mathbf{0})\Delta_{t'}\partial_{t'}C^{2\mathrm{pt}}_{PP}(t',\mathbf{0})-\Delta_t\partial_t C^{2\mathrm{pt}}_{PP}(t,\mathbf{0})\Delta_{t'}C^{2\mathrm{pt}}_{PP}(t',\mathbf{0})}{(E^{2\mathrm{pt}}(\mathbf{p}_i)+E^{2\mathrm{pt}}(\mathbf{p}_f))C^{2\mathrm{pt}}_{PP}(t,\mathbf{p}_i)C^{2\mathrm{pt}}_{PP}(t',\mathbf{p}_f)}\right), \\
R_2'(t,t';\mathbf{0},\mathbf{p}_i) \;\equiv\; & \frac{\Delta_t C^{PV_0P}(t,t';\mathbf{0},\mathbf{p}_i)}{\Delta_t\Delta_{t'}C^{PV_0P}(t,t';\mathbf{0},\mathbf{0})} \\
& \times\left(\frac{-\Delta_t C^{2\mathrm{pt}}_{PP}(t,\mathbf{0})\Delta_{t'}\partial_{t'}C^{2\mathrm{pt}}_{PP}(t',\mathbf{0})-\Delta_t\partial_t C^{2\mathrm{pt}}_{PP}(t,\mathbf{0})\Delta_{t'}C^{2\mathrm{pt}}_{PP}(t',\mathbf{0})}{C^{2\mathrm{pt}}_{PP}(t',\mathbf{p}_i)\left[-\Delta_t\partial_t C^{2\mathrm{pt}}_{PP}(t,\mathbf{0})+E(\mathbf{p}_i)\Delta_t C^{2\mathrm{pt}}_{PP}(t,\mathbf{0})\right]}\right).
\end{aligned}
\tag{102}
$$

Note that $E^{2\mathrm{pt}}(\mathbf{p}) = E^{3\mathrm{pt}}(\mathbf{p})$ at LO. At NLO, their expressions are different, since the zero-mode integrals are different. However, they are numerically very similar to each other with reasonable set-ups of the lattice simulation parameters. In particular, their chiral limit and infinite volume limit are same, as seen in Figure 1. Therefore, these ratios $R_1'(t,t';\mathbf{p}_f,\mathbf{p}_i)$, and $R_2'(t,t';\mathbf{0},\mathbf{p}_i)$ should almost cancel the t and t' dependences, and can directly give the values of $F_V(q_0,\mathbf{q})$.

JLQCD collaboration [14] has employed the latter ratios and found a good plateau for it, extracting a pion charge radius, which is consistent with the experiment.

It should be noted that except for $Z_M^{3\mathrm{pt}}$, which is essentially irrelevant to above ratios, we don't need any zero-mode integrals which could give a complicated combination of Bessel functions. The remaining finite volume effect in $F_V(q_0,\mathbf{q})$ is a perturbatively small correction from the non-zero modes only, and we numerically confirm this expectation in the next subsection.

6–b. Remaining Finite Volume Effects from non-zero modes

Since the dominant finite volume effect from the zero-mode has been eliminated already, the remaining finite volume effect in $F_V(q_0,\mathbf{q})$ is contribution from the non-zero momentum modes, which is expected to be small. In this subsection, we calculate this remaining finite volume effect to the pion one-loop and check this expectation numerically.

All we need to evaluate is

$$
I_{\mu\nu}(q_0,\mathbf{q}) \;=\; \frac{1}{V}\sum_{p\neq 0,q}\frac{-2p_\mu p_\nu}{p^2(p-q)^2}. \tag{103}
$$

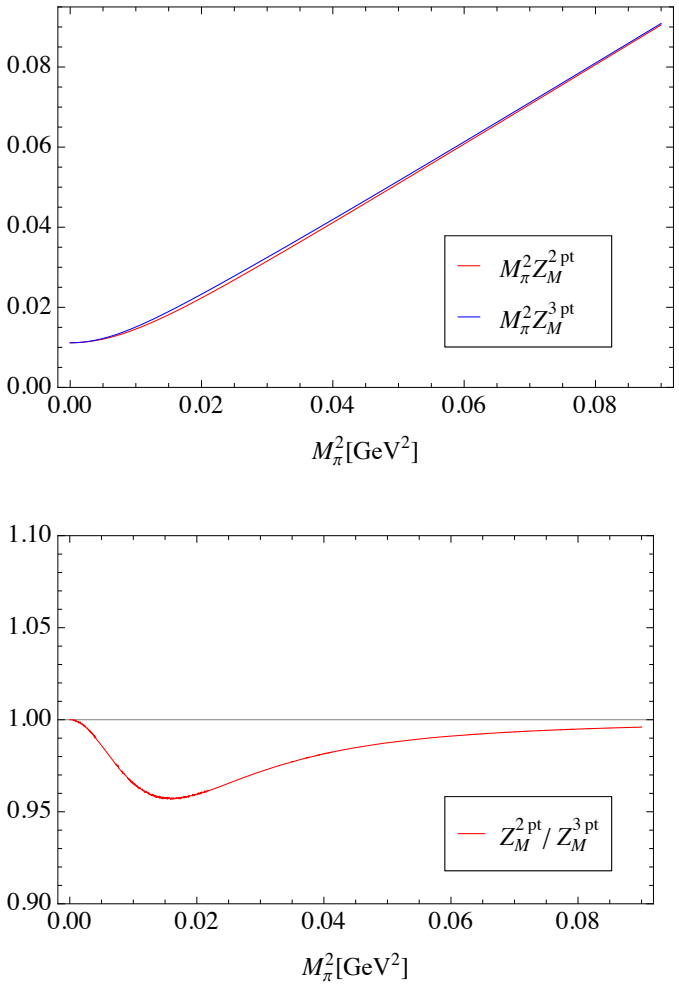

FIG. 1: Numerical estimates for the *pion mass* squared $M_\pi^2 Z_M^{2pt}$ and $M_\pi^2 Z_M^{3pt}$ (top panel) and their ratio Z_M^{2pt}/Z_M^{3pt} (bottom). Here, we use $L = T/2$=2fm, and $F_{\rm eff} = 92.2$ MeV as inputs.

Here and in the following, the terms proportional to q_ν are dropped, which cannot contribute to the final result, since we contract it with a perpendicular 4-momentum vector to q_μ.

We can decompose it as

$$I_{\mu\nu}(q_0, \mathbf{q}) \;=\; \sum_{b_\mu = n_\mu L_\mu} I^b_{\mu\nu}(q_0, \mathbf{q}), \tag{104}$$

where

$$I^b_{\mu\nu}(q_0, \mathbf{q}) \equiv \int \frac{d^4p}{(2\pi)^4} e^{ipb} \frac{-2p_\mu p_\nu}{p^2(p-q)^2}. \tag{105}$$

Since $I^{b=0}(q_0, \mathbf{q})$ is the infinite volume limit of $I_{\mu\nu}(q_0, \mathbf{q})$, we can write the finite volume

correction as

$$\Delta I_{\mu\nu}(q_0, \mathbf{q}) \;=\; \sum_{b\neq 0} I^b_{\mu\nu}(q_0, \mathbf{q}). \tag{106}$$

In the standard way, each contribution $I^b_{\mu\nu}(q_0, \mathbf{q})$ can be computed as

$$\begin{aligned} I^b_{\mu\nu}(q_0, \mathbf{q}) \;&=\; 2\frac{\partial}{\partial b^\mu}\frac{\partial}{\partial b^\nu}\int_0^1 dx e^{ixbq}\int \frac{d^4p}{(2\pi)^4}\frac{e^{ipb}}{(p^2+\Delta)^2} \\ &=\; -\frac{1}{4\pi^2}\int_0^1 dx e^{ixbq}\left[\frac{\delta_{\mu\nu}}{|b_\mu|}\sqrt{\Delta}K_1(\sqrt{\Delta}|b_\mu|) - \frac{b_\mu b_\nu}{|b_\mu|^2}\Delta K_2(\sqrt{\Delta}|b_\mu|)\right], \end{aligned} \tag{107}$$

with $\Delta = x(1-x)q^2$, and the i-th modified Bessel function $K_i(z)$. Here, we have dropped a term proportional to $q_\mu b_\nu$, since it is proportional to q_ν after performing the summation over b_ν.

In the case of $b_0 = 0$, the above form is numerically evaluated in straight forward way. While $b_0 \neq 0$ case, we need a special care since analytical continuation of the results with respect to q_0 is necessary. Here we make use of the following inequality

$$\left|\int_0^1 dx e^{i\alpha} f(x)\right| < \left|\int_0^1 dx |e^{i\alpha}| f(x)\right| = \left|\int_0^1 dx f(x)\right|, \tag{108}$$

in Eq. (107). Namely the oscillating factor $\exp(ixb_0q_0)$ is neglected. Then there is no subtlety within the analytic continuation of q_0 since the Bessel functions go to zero in the limit $|q_0| \to \infty$ with any complex phase. Note here that the real part of $\sqrt{\Delta}$ is always positive. We think that this *over-estimation* does not affect the result very much, since the size of temporal direction is usually larger than that of the spacial direction by a factor of 2 or 3, and therefore, the contribution from $b_0 \neq 0$ is much smaller from the beginning.

Taking $\mu = 0$ direction the remaining finite volume correction in $F_V(q_0, \mathbf{q})$ can be computed as

$$\begin{aligned} \Delta F_V(q_0, \mathbf{q}) \;&\equiv\; F_V(q_0, \mathbf{q}) - F_V^\infty(q_0, \mathbf{q}) \\ &=\; -\frac{N_f}{2F_{\text{eff}}^2}\left(\Delta l(q_0, \mathbf{q}) - l_{00}\right), \end{aligned} \tag{109}$$

where

$$\Delta l(q_0, \mathbf{q}) \;=\; -\frac{1}{4\pi^2}\sum_{b_\mu}\int_0^1 dx e^{ix\mathbf{b}\cdot\mathbf{q}}\left[\frac{\sqrt{\Delta}}{|b_\mu|}K_1(\sqrt{\Delta}|b_\mu|) - \frac{b_0^2}{|b_\mu|^2}\Delta K_2(\sqrt{\Delta}|b_\mu|)\right]. \tag{110}$$

Note that $\Delta l(0,\mathbf{0}) = l_{00}$.

Our numerical estimates for $\Delta F_V(q_0,\mathbf{q})$ at $L = T/2 = 2,3,4\,\mathrm{fm}$ are presented in Fig. 2. Here, we denote $q^0 = i\left(\sqrt{\mathbf{p}_f^2 + M_\pi^2} - \sqrt{\mathbf{p}_i^2 + M_\pi^2}\right)$, assuming the dispersion relation of the pion energy, $\mathbf{q} = \mathbf{p}_f - \mathbf{p}_i$, and choose $M_\pi = 135\mathrm{MeV}$, $F_{\mathrm{eff}} = 92.2\mathrm{MeV}$, as inputs. The zig-zag behavior may be due to the lack of the rotational symmetry on the lattice. Since $F_V^\infty(q^2)$ is an $\mathcal{O}(1)$ quantity, our result shows the remaining finite volume effects is around a few % already at $L = 3\,\mathrm{fm}$, even when $m_\pi L < 1$. Strictly speaking, this statement is correct for small q^2 region, since ChPT is not valid for large q^2 region. However, the important region is small q^2 region where the finite volume effects are generally large and our analysis is valid, and there, the finite volume effects are suppressed to a few percent level. Thus, we can conclude that our method does control the finite volume effects.

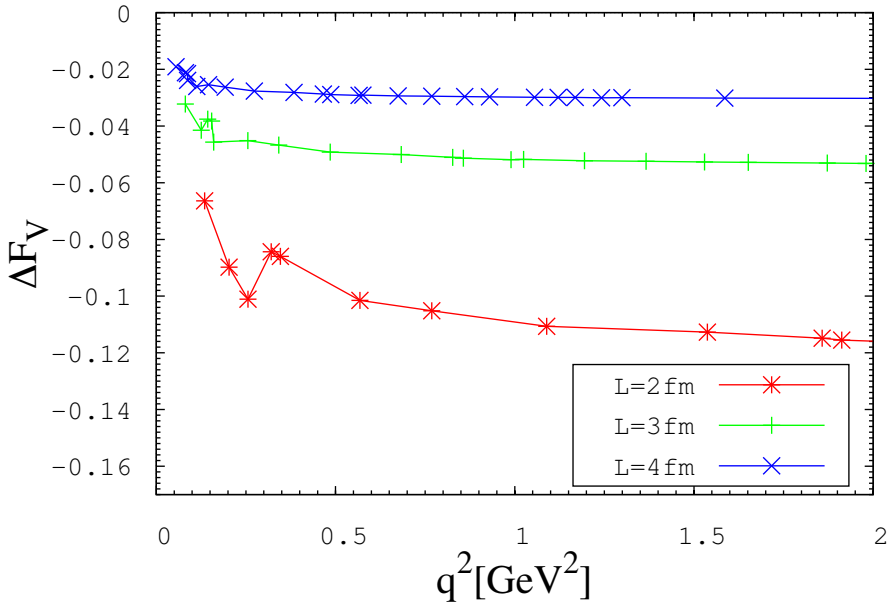

FIG. 2: Numerical estimates for ΔF_V.

7. SUMMARY AND DISCUSSION OF PART I

In Part I, we have studied finite volume effects on the electro-magnetic pion form factor in the ϵ regime. The pseudoscalar-vector-pseudoscalar three point function has been calculated in the ϵ expansion of chiral perturbation theory to the next-to-leading order.

The dominant finite volume effects, which come from the zero-mode of the pions can

be removed by two simple manipulations: by inserting non-zero momentum to relevant operators (or making a subtraction at different time correlators) and taking a appropriate ratio of them. After these manipulations, one can safely extract the electro-magnetic pion form factor for which the remaining finite volume correction from the non-zero modes is suppressed to a few percent level already at $L = 3\,\mathrm{fm}$ even in the ϵ regime (see Figure 2).

It is important to note that our analysis has been done without using any special features of the ϵ expansion, and the dominance of the zero-mode contribution is expected to be a common feature of finite volume effects in any regime of QCD. Therefore, our method can be useful for simulations in the p regime, including the ones with twisted boundary conditions [36, 37]. We also expect a wide application to other quantities like form factors of heavier hadrons.

Part II

Computation of form factors of D meson with chiral fermions

8. INTRODUCTION TO PART II

Next, we consider the form factors of D meson semileptonic decays. The previous lattice works for D meson semileptonic decays [38–41] all use a lattice fermion formulation which violates the chiral symmetry. However, this violation could give a sizable discretization effects and be a source of a systematic error. JLQCD collaboration employs with the Möbius domain-wall fermion, which preserves a good chiral symmetry on lattice, and perform simulations with fine lattice spacing ~ 0.08 fm. Since we simulate with finer lattice spacing ~ 0.04 fm, it can be expected that errors from a finite lattice spacing will be better controlled.

As we have mentioned in Sec. 1, it is important to precisely test the standard model of particle physics. In particular, the Cabibbo-Kobayashi-Maskawa matrix [3, 4] is important to check since physics beyond the standard model are most likely to appear. In the standard model, flavor can change, at tree level, only through charged currents interactions. This is the consequence of the unitarity of the CKM matrix. Therefore, we can test the standard model by checking how well the CKM matrix satisfies the unitarity relation. It is therefore important to precisely determine a value of the CKM matrix elements.

Among the CKM matrix elements, the elements $|V_{cs}|$ and $|V_{cd}|$ can be determined from the semileptonic weak decays of the D meson, $D \to \pi\ell\nu$, where ℓ and ν denote a lepton and its neutrino, respectively. From the standard model analysis, the differential decay rate of the $D \to \pi\ell\nu$ in the rest frame of the D meson reads,

$$\frac{\Gamma(D \to \pi\ell\nu)}{dq^2} = \frac{G_F^2 |\mathbf{p}_\pi|^3}{24\pi^3} |V_{cd}|^2 |f_+^{D\to\pi}(q^2)|^2, \tag{111}$$

where $q^2 = (p_D - p_\pi)^2$ is the momentum transfer, G_F is the Fermi constant, and $\mathbf{p}_\pi$ is the three momentum of the daughter pion (π). Here we have neglected the term proportional to the lepton mass squared. Note that, the same relation holds also for $D \to K$ if one replace

π and $|V_{cd}|$ by K and $|V_{cs}|$, respectively. In the past decade, these decay processes have been precisely measured and determined its dependence on q^2 by several experiments [44–46].

However, experiments don't give us the CKM matrix elements V_{cd} itself but give $|V_{cd}|^2|f_+^{D\to\pi}(q^2)|^2$ as a function of q^2. The form factor $f_+^{D\to\pi}(q^2)$ can be obtained from lattice QCD calculation, and we can determine the CKM matrix elements by combining experimental results with lattice QCD analysis.

Currently, the most precise lattice results for $f_+(0)$ is given by the HPQCD Collaboration [38, 39]. Combining these results with the corresponding experimental results from the Heavy Flavor Averaging Group [42], the CKM matrix elements can be determined as

$$|V_{cd}| = 0.214(9)_{\rm LQCD}(3)_{\rm expt}, \quad |V_{cs}| = 0.977(14)_{\rm LQCD}(7)_{\rm expt}. \tag{112}$$

Note that lattice QCD results have the errors of several times larger than that of experiments and give the limit of accuracy of $|V_{cd}|$ and $|V_{cs}|$ determined from semileptonic decays. Thus, lattice QCD is required to compute the CKM matrix elements within errors of a level at the experimental errors.

To do that, lattice QCD must precisely calculate the form factor $f_+^{D\to\pi}(q^2)$. It appears together with another form factor $f_-^{D\to\pi}(q^2)$ or $f_0^{D\to\pi}(q^2)$ as a coefficient in a standard decomposition of the $D\to\pi$ (or K) hadronic matrix element,

$$\begin{aligned}\langle\pi(p_\pi)|V_\mu|D(p_D)\rangle &= f_+^{D\to\pi}(q^2)(p_D+p_\pi)_\mu + f_-^{D\to\pi}(q^2)(p_D-p_\pi)_\mu \\ &= f_+^{D\to\pi}(q^2)\left[p_D+p_\pi-\frac{m_D^2-m_\pi^2}{q^2}q\right]_\mu + f_0^{D\to\pi}(q^2)\frac{m_D^2-m_\pi^2}{q^2}q_\mu,\end{aligned} \tag{113}$$

with $V_\mu = \bar{c}\gamma_\mu d$. The form factors can be extracted by combining the matrix elements of spatial component with that of temporal component (see later). Note that two form factors in second line obey the kinematical condition $f_+(0) = f_0(0)$.

In this part, we compute the $D\to\pi$ and $D\to K$ form factors from lattice QCD simulation employed with Möbius domain-wall fermion for both heavy and light quarks by JLQCD Collaboration.

9. METHOD

In this section, we explain our method to calculate the form factors from lattice simulations. Although the form factors can be extracted from the hadronic matrix elements, it

is the correlation functions that lattice simulations directly compute. Thus, we first show how the hadronic matrix elements can be related to the correlation functions. Then, we will present a way to calculate the form factors from the correlation functions.

The three- and two- point correlation functions are calculated as

$$C_\mu^{D\to\pi}(\Delta t,\Delta t';\mathbf{p}_D,\mathbf{p}_\pi) \equiv \frac{1}{V}\sum_{\mathbf{x},t}\sum_{\mathbf{x}',\mathbf{x}''}\left\langle \mathcal{O}_\pi(\mathbf{x}'',t+\Delta t+\Delta t')V_\mu(\mathbf{x}',t+\Delta t)\mathcal{O}_D^\dagger(\mathbf{x},t)\right\rangle \times e^{-i\mathbf{p}_D(\mathbf{x}''-\mathbf{x}')}e^{-i\mathbf{p}_\pi(\mathbf{x}'-\mathbf{x})}, \tag{114}$$

$$C^{D(\pi)}(\Delta t;\mathbf{p}_{D(\pi)}) \equiv \frac{1}{V}\sum_{\mathbf{x},t}\sum_{\mathbf{x}'}\left\langle \mathcal{O}_{D(\pi)}(\mathbf{x}',t+\Delta t)\mathcal{O}_{D(\pi)}^\dagger(\mathbf{x},t)\right\rangle e^{-i\mathbf{p}_{D(\pi)}(\mathbf{x}'-\mathbf{x})}, \tag{115}$$

with the meson interpolating operator $\mathcal{O}(\mathbf{x},t)=\sum_{\mathbf{x}'}\phi(\mathbf{x}')\bar{q}(\mathbf{x}+\mathbf{x}',t)\gamma_5 q(\mathbf{x},t)$ where $\phi(\mathbf{x}')$ represents the Gaussian smearing operator: $(1-(\alpha/N)\Delta)^N$ with the Laplacian Δ, $\alpha=5.0$ and $N=50$. For large Δt and $\Delta t'$, asymptotic behaviors of above correlation functions are written as

$$C_\mu^{D\to\pi}(\Delta t,\Delta t';\mathbf{p}_D,\mathbf{p}_\pi) \xrightarrow{\text{large }\Delta t,\ \Delta t'} \langle\pi(p_\pi)|V_\mu|D(p_D)\rangle\frac{Z_D(p_D)^*Z_\pi(p_\pi)}{4E_DE_\pi}e^{-E_D\Delta t}e^{-E_\pi\Delta t'}, \tag{116}$$

$$C^{D(\pi)}(\Delta t;\mathbf{p}_{D(\pi)}) \xrightarrow{\text{large }\Delta t} \frac{\left|Z_{D(\pi)}(p_{D(\pi)})\right|^2}{2E_{D(\pi)}}e^{-E_{D(\pi)}\Delta t}, \tag{117}$$

where $E_{D(\pi)}=\sqrt{m_{D(\pi)}^2+\mathbf{p}_{D(\pi)}^2}$ denotes the energy of D or π meson, for which we assume the dispersion relation. The factor $Z_{D(\pi)}(p_{D(\pi)})=\langle D(\pi)(t=0)|D(\pi)(p_{D(\pi)})\rangle$ represents an overlap with state at $t=0$, which will automatically cancel in our extraction of the form factors. It is important to note that our desired hadronic matrix element appears in Eq. (116), and the other kinematical factors are almost identical to Eq. (117). In the literature, one can find some ratios of the two- and three- functions (see [43] for example), which cancel the kinematical factors and give the hadronic matrix element.

In this study, however, we first consider a quantity given by dividing the correlation function by its exponential factor and extract its asymptotic behavior at large separations. We define

$$A_\mu^{D\to\pi}(\mathbf{p}_D,\mathbf{p}_\pi) \equiv \left.\frac{C_\mu^{D\to\pi}(\Delta t,\Delta t';\mathbf{p}_D,\mathbf{p}_\pi)}{\exp(-E_D\Delta t-E_\pi\Delta t')}\right|_{\text{large }\Delta t,\ \Delta t'}, \tag{118}$$

$$B^{D(\pi)}(\mathbf{p}_{D(\pi)}) \equiv \left.\frac{C^{D(\pi)}(\Delta t;\mathbf{p}_{D(\pi)})}{\exp(-E_{D(\pi)}\Delta t)}\right|_{\text{large }\Delta t}. \tag{119}$$

Note that these factors have no time dependence for sufficiently large Δt or $\Delta t'$. Considering the asymptotic behavior in Eqs. (116) and (117), the desired hadronic matrix elements can be computed as

$$R_\mu^{D\to\pi}(\mathbf{p}_D, \mathbf{p}_\pi) \equiv 2Z_V\sqrt{E_D E_\pi}\sqrt{\frac{\left|A_\mu^{D\to\pi}(\mathbf{p}_D, \mathbf{p}_\pi)\right|^2}{B^D(\mathbf{p}_D)B^\pi(\mathbf{p}_\pi)}} = \langle\pi|V_\mu|D\rangle, \tag{120}$$

where Z_V is the renormalization factor of the vector current, whose value is calculated non-perturbatively in [47] as $Z_V = 0.951(4)$ at $\beta = 4.17$.

In this procedure to extract the hadronic matrix elements, we see plateaus of the r.h.s. of Eqs. (118) and (119) at large separations and perform the constant fit. Since we use information of some data points in this step, this method have a statistical advantage compared to the other methods where one or two data points are used. We expect that this can help to improve accuracy.

We are now ready to extract the form factors. For $q^2 < q^2_{\rm max} = (m_D - m_\pi)^2$, we can compute the form factors through the following relations of these R's:

$$f_+^{D\to\pi}(q^2) = \frac{(E_D - E_\pi)\, R_k^{D\to\pi}(\mathbf{p}_D, \mathbf{p}_\pi) - (p_D - p_\pi)^k\, R_4^{D\to\pi}(\mathbf{p}_D, \mathbf{p}_\pi)}{2E_D\, p_\pi^k - 2E_\pi\, p_D^k}, \tag{121}$$

$$f_-^{D\to\pi}(q^2) = \frac{(E_D + E_\pi)\, R_k^{D\to\pi}(\mathbf{p}_D, \mathbf{p}_\pi) - (p_D + p_\pi)^k\, R_4^{D\to\pi}(\mathbf{p}_D, \mathbf{p}_\pi)}{2E_\pi\, p_D^k - 2E_D\, p_\pi^k}, \tag{122}$$

$$f_0^{D\to\pi}(q^2) = f_+^{D\to\pi}(q^2) + f_-^{D\to\pi}(q^2)\frac{q^2}{(m_D^2 - m_\pi^2)}, \tag{123}$$

where k denotes the k-th spatial component. At $q^2 = q^2_{\rm max}$, one can access only to $f_0(q^2_{\rm max})$, which can be given by

$$\frac{R_4^{D\to\pi}(\mathbf{0}, \mathbf{0})}{m_D + m_\pi} = f_0^{D\to\pi}(q^2_{\rm max}). \tag{124}$$

Note that all the relations in this section hold for the $D \to K$ case by replacing π by K.

10. LATTICE SET UP

We use the 2+1-flavor gauge ensembles generated with the Symanzik gauge action and the Möbius domain-wall fermion action with three times stout smearing of the link variables. In this work, we use the lattice of size $L^3 \times T(\times L_s) = 32^3 \times 64(\times 12)$ at $\beta = 4.17$, of which the lattice cut-off is estimated to be 2.453(4) GeV using the Wilson flow.

β	a^{-1} [GeV]	$(L/a)^3 \times T/a$	am_s	am_{ud}
4.17	2.453(4)	$32^3 \times 64$	0.030	0.007
4.17	2.453(4)	$32^3 \times 64$	0.030	0.012
4.17	2.453(4)	$32^3 \times 64$	0.030	0.019
4.17	2.453(4)	$32^3 \times 64$	0.040	0.0035
4.17	2.453(4)	$32^3 \times 64$	0.040	0.007
4.17	2.453(4)	$32^3 \times 64$	0.040	0.012
4.17	2.453(4)	$32^3 \times 64$	0.040	0.019
4.17	2.453(4)	$48^3 \times 96$	0.040	0.0035
4.35	3.610(9)	$48^3 \times 96$	0.018	0.0042
4.35	3.610(9)	$48^3 \times 96$	0.018	0.0080
4.35	3.610(9)	$48^3 \times 96$	0.018	0.0120
4.35	3.610(9)	$48^3 \times 96$	0.025	0.0042
4.35	3.610(9)	$48^3 \times 96$	0.025	0.0080
4.35	3.610(9)	$48^3 \times 96$	0.025	0.0120
4.47	4.496(9)	$64^3 \times 128$	0.015	0.0030

TABLE I: All simulation parameters used in lattice simulations by JLQCD collaboration. Parameters which we use in this analysis are written in red color.

The simulation parameters are summarized in Table 10. Among these parameters, parameters in red are used in this analysis. We use three values of the up and down quark masses, $am_{ud} = 0.007,\ 0.012$ and 0.019. The strange quark mass is set to be $am_s = 0.04$ for all m_{ud}. The corresponding pion mass is 308, 399, and 498 MeV, respectively. On each ensemble, 100 configurations are sampled from 10,000 HMC trajectories and 2–8 different source points are taken to improve statistics. We estimate the error by the jackknife method with bin-size 4.

The same ensembles are also used for a calculation of the charmed meson decay constants f_D and f_{D_s} [48]. We found that the discretization effect is not significant for these quantified by comparing the results with those on finer lattices at $\beta = 4.35$ and 4.47.

11. NUMERICAL RESULTS

First, we consider the dependence of the r.h.s. of Eqs. (118) and (119) on time separations to extract the factors $A_\mu^{D\to\pi}(\mathbf{p}_D, \mathbf{p}_\pi)$ and $B^{D/\pi}(\mathbf{p}_{D/\pi})$. Typical results are shown in Figs. 3 and 4. In Fig. 4, the horizontal axis Δt represents the temporal position of current operator V_μ, and the source and sink operators are set to $t = 0$ and $t + \Delta t + \Delta t' = 28$, respectively. As we have already mentioned, we assume that the simple dispersion relation for the energy of mesons is hold. One can see that there are reasonable plateaus in Fig. 4, and we observe similar reasonable plateau on each ensemble. From these plateau, we extract the factors $A_\mu^{D\to\pi}(\mathbf{p}_D, \mathbf{p}_\pi)$ and $B^{D/\pi}(\mathbf{p}_{D/\pi})$ by a constant fit, which is shown by a horizontal line in Fig. 4.

Having the ratio of the factors $A_\mu^{D\to\pi}(\mathbf{p}_D, \mathbf{p}_\pi)$ and $B^{D/\pi}(\mathbf{p}_{D/\pi})$ in Eq. (120), we compute the form factors through Eqs. (121)–(124). In Fig. 5, we show our result for the form factors $f_+(q^2)$ or $f_0(q^2)$ at three different pion masses as a function of the momentum transfer q^2. The solid curve is a simple pole model fit of the experimental data by CLEO Collaboration [44] (with an input for $|V_{cd(s)}|$ from PDG [10]). We observe that our data shows a reasonable agreement with the solid curve and suggests a mild m_π dependence of $f_+(q^2)$ which indicates to be bale to take the chiral limit. Our data of $D \to \pi$ deviates from the solid curve at large q^2. Similar behavior can be seen in other lattice simulations, for example Fig. 4 in [41]. This may be due to heavy simulated pion masses or the finite volume effects. However, we do not confirm this point yet and need a more detailed analysis.

Next, we determine the q^2 dependence of the form factors $f_+(q^2)$ to compute a value at zero momentum transfer $f_+(0)$ which is conventionally used to extract the CKM matrix elements $|V_{cd}|$ and $|V_{cs}|$. In the literature, several parametrizations of the form factors can be found. In this work, we use the parametrization based on the Vector Meson Dominance (VMD) hypothesis [50–55]:

$$f_+^{\rm fit}(q^2) \;=\; \frac{f_+(0)}{1 - q^2/m_V^2} \times (\text{Polynomial of } q^2), \tag{125}$$

where the vector meson pole mass m_V is the m_{D^*} and $m_{D_s^*}$ in the case of $D \to \pi$ and $D \to K$, respectively. We use m_V as an input whose value is measured at simulated pion masses : m_{D^*} =2.033(14), 2.064(9), and 2.065(7) [GeV], and $m_{D_s^*}$ = 2.127(4), 2.123(4), and 2.127(4) [GeV], for $m_\pi = 308, 399$, and 498 [MeV], respectively.

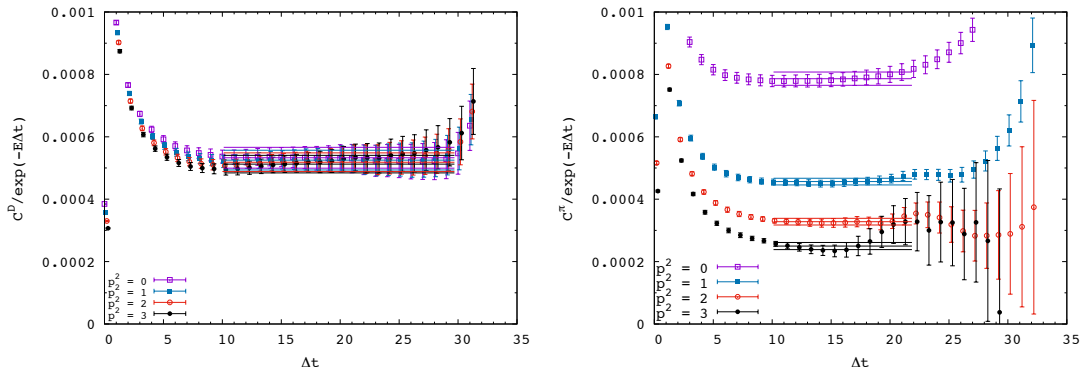

FIG. 3: The factor $B^D(\mathbf{p}_D)$ (left) and $B^\pi(\mathbf{p}_\pi)$ (right). The horizontal axis denotes the temporal distance of two-point function. Data with four different momenta are shown. The corresponding pion mass is 399 MeV. The factor $B^{D/\pi}(\mathbf{p}_{D/\pi})$ is determined from the plateaus, as shown by the horizontal lines.

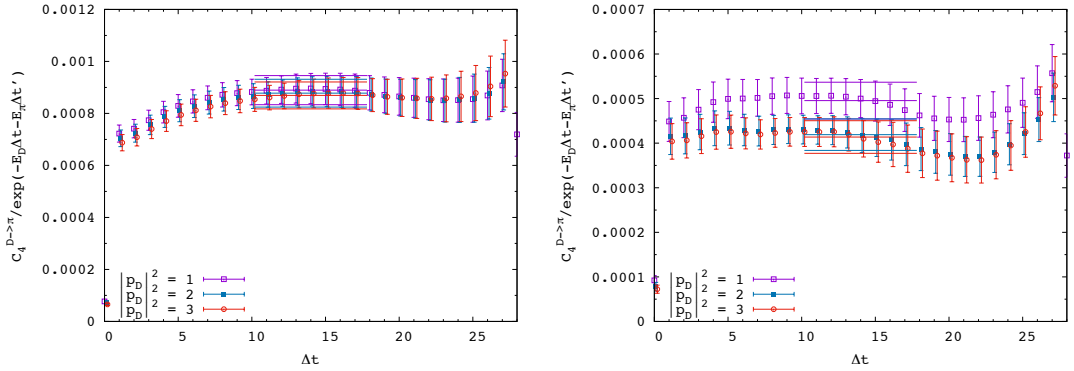

FIG. 4: $A_\mu^{D\to\pi}(\mathbf{p}_D, \mathbf{p}_\pi)$ with $\mathbf{p}_\pi = \mathbf{0}$ (left) or $\mathbf{p}_\pi \neq \mathbf{0}$ (right). Data for three different momenta $\mathbf{p}_D$ of D meson are plotted. The horizontal axis denotes the temporal position of the current operator. The corresponding pion mass is 399 MeV. Source and sink operators are set at $t = 0$ and $t + \Delta t + \Delta t' = 28$, respectively.

The "Polynomial of q^2" in Eq. (125) is set to three types: 1, $1 + aq^2$, and $1 + aq^2 + b(q^2)^2$. We fit these three functions to our data and determine the unknown fit parameters $f_+(0)$, a and b. Note that the case of 1 is just the simple pole model which is used to obtain the solid curve in Fig. 5, though m_V is also considered as the fit parameters there. Our results are shown in Fig. 6. The value of χ^2/d.o.f. is 1.9, 0.25 and 0.045 for 1, $1 + aq^2$, and $1 + aq^2 + b(q^2)^2$, respectively (for $D \to \pi$ at $m_\pi = 399$ MeV). In Fig. 6, our fit results with the simple pole model are represented by purple dashed lines, and one can see that this model fails to describe the data at large q^2. Since the results for the parameter b tend to be consistent with zero with a small χ^2/d.o.f., we normally use the fit function VMD $* (1 + aq^2)$

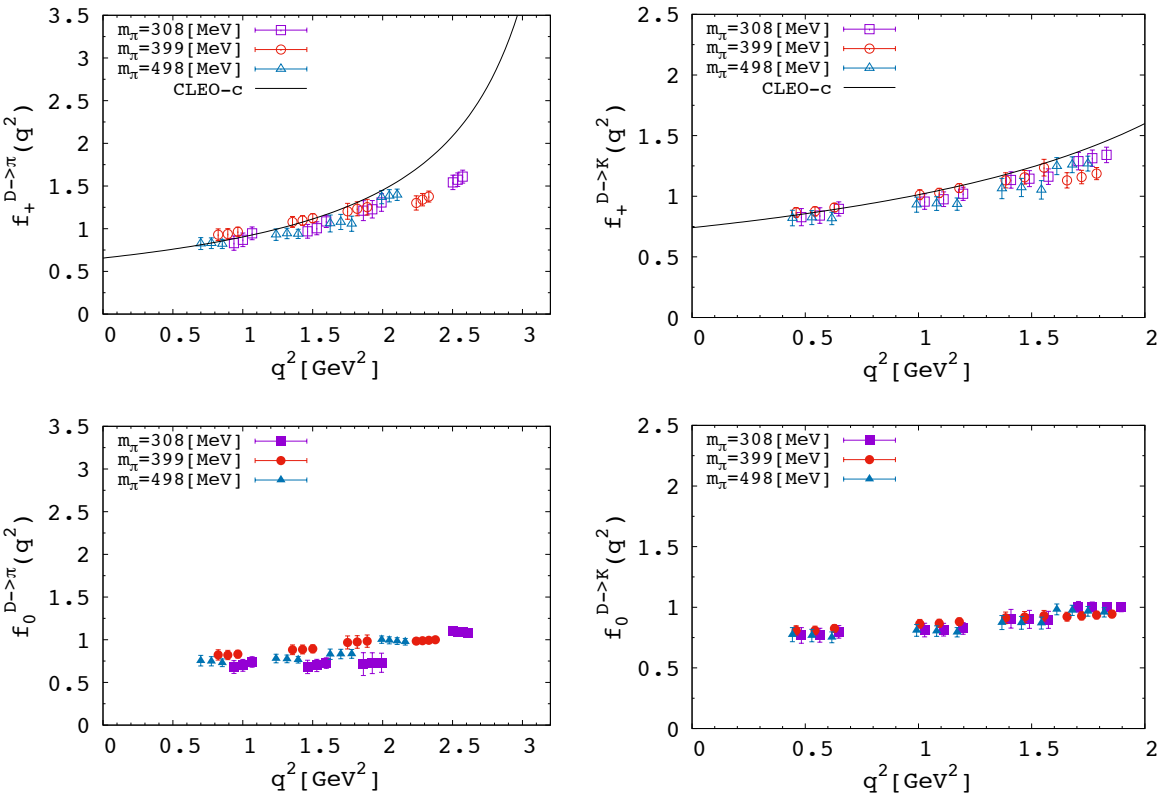

FIG. 5: q^2 dependence of the form factors $f_+(q^2)$ (upper plot) and $f_0(q^2)$ (lower plot) of $D \to \pi$ (left) and $D \to K$ (right). Different colors represent different pion masses. The solid curve in upper plot shows a single pole fit of the experimental data by CLEO-c [44].

in the following analysis.

Next step is to consider a chiral extrapolation of $f_+(0)$. Since our simulated pion masses are all heavier than the physical pion mass, our data for $f_+(0)$ should be extrapolated to a point at the physical pion mass. As we have seen in Fig. 5, our results for the form factors show a mild m_π dependence. Especially, our results for $f_+(0)$ with the fit function $\mathrm{VMD} * (1 + aq^2)$ are shown in Fig. 7 by the green points, and these are consistent with each other within our error-bars. We therefore determine the $f_+(0)$ at the physical pion mass by a simple constant fit, and this result is represented by the green solid lines in Fig. 7. Our results are consistent with the current world average of lattice results by FLAG [5] (or [38, 49]), which is shown by the black points.

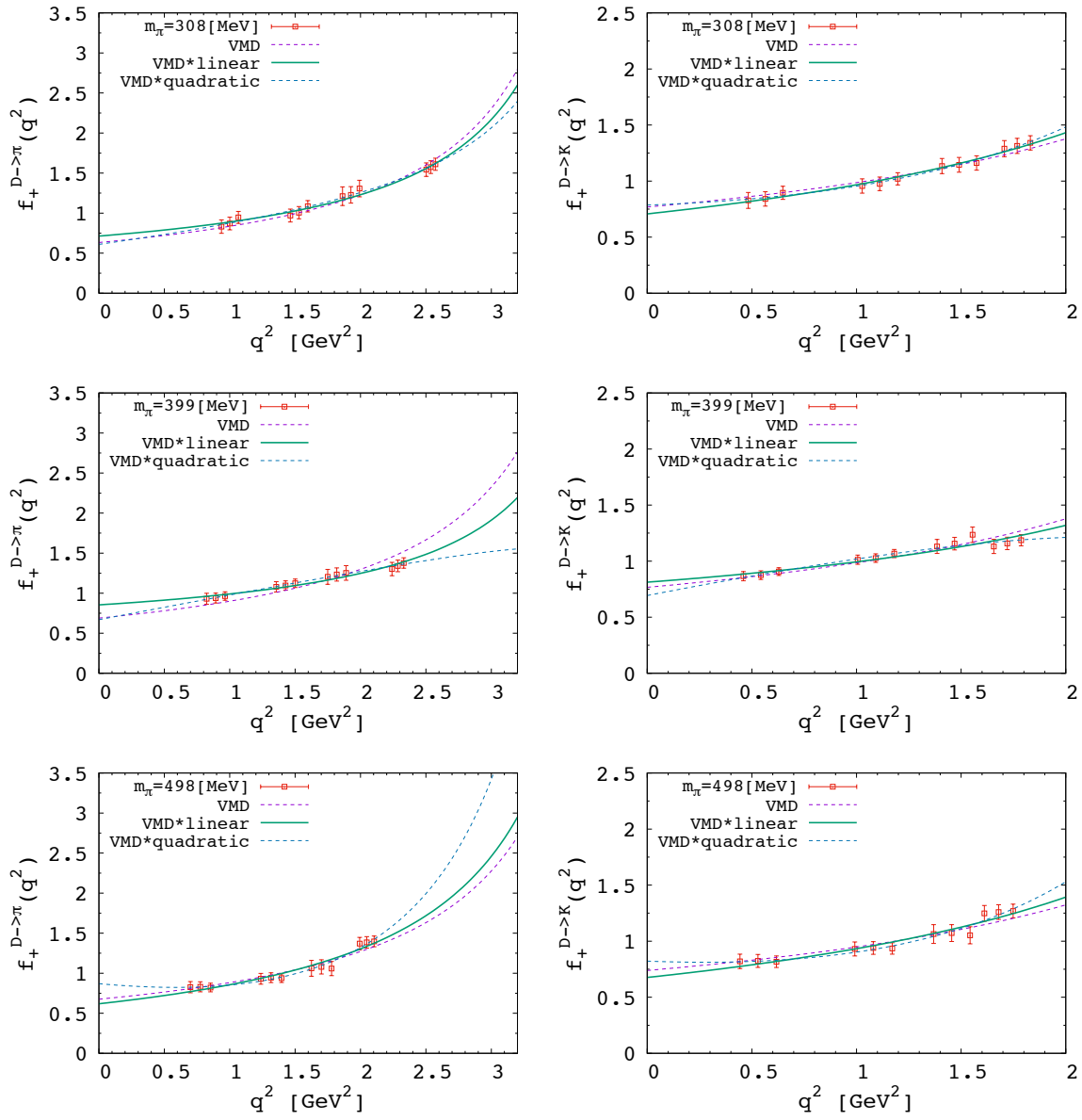

FIG. 6: Our fit results to $f_+(q^2)$ of $D \to \pi$ (left) and $D \to K$ (right). The simulated pion masses are 308, 399 and 498 MeV. Curves represent the fits motivated by the VMD hypothesis. See the text for more details.

12. SUMMARY AND DISCUSSION OF PART II

In this work, we compute the form factors for the D meson semileptonic decays by lattice QCD with chiral fermions for both heavy and light quarks. Our current results for the form

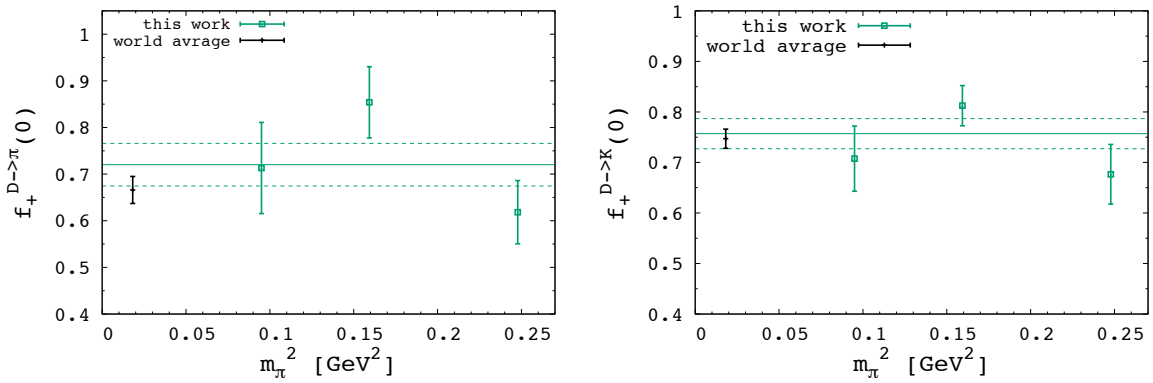

FIG. 7: $f_+(0)$ of $D \to \pi$ (left) and $D \to K$ (right). The black points are the values by FLAG [5] (or [38, 49]). The result with the fit function $1 + aq^2$ as "Polynomial" in Eq. (125) are shown.

factors at zero momentum transfer $f_+(0)$ at the physical pion mass are

$$f_{+\,\mathrm{phys}}^{D\to\pi}(0) = 0.720\,(45)_{\mathrm{stat}}(41)_{\mathrm{sys}}, \qquad f_{+\,\mathrm{phys}}^{D\to K}(0) = 0.757(29)_{\mathrm{stat}}(02)_{\mathrm{sys}}, \tag{126}$$

where the first and second error is statistical and systematic error, respectively. We compute these results with the fit function VMD $*\,(1 + aq^2)$ and estimate the systematic error from the difference of the results with various fit functions. Combined with the results by CLEO Collaboration [44], $f_+^{D\to\pi}(0)|V_{cd}| = 0.148$ and $f_+^{D\to K}(0)|V_{cs}| = 0.721$, our result Eq. (126) yields the results for the CKM matrix elements as $|V_{cd}| = 0.205(12)_{\mathrm{stat}}(11)_{\mathrm{sys}}$, $|V_{cs}| = 0.952(36)_{\mathrm{stat}}(02)_{\mathrm{sys}}$. These values are consistent with those in PDG [10], $|V_{cd}| = 0.22522(61)$, $|V_{cs}| = 0.97343(15)$. Our results for the CKM matrix elements have the error which is larger than that of Eq. (112) by a factor around 2. There may be sveral directions to decrease these errors.

One possible way is making use of the kinematical condition $f_+(0) = f_0(0)$. Although it is not shown in this theses, we have also calculated the scalar form factor $f_0(q^2)$ as well as $f_+(q^2)$. If we perform a fit to results of both $f_+(q^2)$ and $f_0(q^2)$ with the constraint $f_+(0) = f_0(0)$ in determination of a q^2 dependence, the errors on $f_+(0)$ (and then on the CKM matrix elements) should become smaller.

Another one is using another parametrization of the form factors. Commonly used one is the so-called z-expansion (also known as the series expansion) [56]. In that expansion, q^2 is converted to a new parameter z which satisfy the $|z| < 1$ for the semileptonic energy

region, and the form factors are expanded in this parameter z with a good convergence. This parametrization would help to reduce the systematic error.

It would be also helpful to use results at other q^2 points. Although $f_+(0)$ is conventionally used to compute the CKM matrix elements, one can extract the CKM matrix elements from an experimental result at each experimental q^2 bin. We integrate the form factors obtained from lattice QCD over an experimental q^2 bin and divide the experimental results at corresponding q^2 bin by the lattice results to compute the CKM matrix elements. Then, the final result can be computed by putting together all/some CKM results at each experimental q^2 bin. This procedure should give us a more accurate result, since more information is used compared to our calculation where only data at $q^2 = 0$ has been used.

We should also consider the continuum limit. Although, we use data of only $\beta = 4.17$, JLQCD Collaboration has configurations of other β's. It is therefore important to observe a dependence of the results on lattice spacing. This is our future work.

13. CONCLUSIONS

In this thesis, we have calculated the meson form factors, and studied on systematic errors of lattice QCD numerical calculations.

In Part I, we have computed the pseudoscalar-vector-pseudoscalar three point function within the ϵ expansion of ChPT and extract the electro-magnetic form factors of pions. From that analysis, we have shown that the finite volume effects can be suppressed to a few percent already level at $L = 3$ fm by applying the following manipulations to correlators:

1. inserting non-zero momenta to relevant operators (or taking a subtraction of the correlators at different source points when one or two of the inserted momenta are zero).

2. taking ratios of them.

With these steps, one can construct a quantity which automatically cancels the dominant finite volume effects comes from pion's zero-momentum mode contributions. This cancellation induced by above manipulations is based on the fact that pion's zero momentum mode gives the dominant finite volume effects and is space-time independent constant mode. Since this feature of pion's zero-momentum mode is universal, we can expect a wide application of our method.

In Part II, we have calculated the form factors of D meson semileptonic decays from lattice QCD simulations employed with chiral fermions by JLQCD Collaboration. They employ with the Möbius domain-wall fermion formalism with keeping a lattice spacing small $\sim 0.04, 0.06$, and 0.08 fm. This is the first lattice result for the form factors of D meson semileptonic decays with chiral fermions. As a result, we have obtained $f_{+\,\mathrm{phys}}^{D\to\pi}(0) = 0.720\,(45)_{\mathrm{stat}}(41)_{\mathrm{sys}}$ and $f_{+\,\mathrm{phys}}^{D\to K}(0) = 0.757(29)_{\mathrm{stat}}(02)_{\mathrm{sys}}$. Combining with the experimental results by CLEO [44], the CKM matrix elements are given as $|V_{cd}| = 0.205(12)_{\mathrm{stat}}(11)_{\mathrm{sys}}$, $|V_{cs}| = 0.952(36)_{\mathrm{stat}}(02)_{\mathrm{sys}}$.

Acknowledgement

I would like to show my greatest appreciation to Hidenori Fukaya for his numerous support, polite guidance, invaluable discussions. My graduate school life can not be without his long-term considerable supports about everything. I am deeply grateful to Yutaka Hosotani for providing me the irreplaceable opportunity to study and enjoy the physics in Osaka. I owe a very important debt to my precious collaborators, Yong-Gwi Cho, Shoji Hashimoto, Takashi Kaneko, and Jun-ichi Noaki for their valuable efforts and useful discussions. My heartfelt appreciation goes to Tetsuya Onogi, Satoshi Yamaguchi and Akio Tomiya. I got a lot of help from their fruitful advice and discussions. Special thanks to Aya Kagimura, Ryo Yamamura and Carsten Fritzner Frøstrup. Valuable discussions and seminars with them gave me deep understanding and a lot of knowledge. I would like to offer my special thanks to my colleagues, Tetsuya Enomoto, Shuichiro Funatsu, Nobuhiko Misumi, Akihiko Sonoda, and Kengo Yamamoto for their moral support. I would like to express cordial gratitude to HET members, especially, Koji Hashimoto and Keiko Takeda, for their continuing enormous support.

Numerical simulations are performed on IBM System Blue Gene Solution at the High Energy Accelerator Research Organization (KEK) under a support of its Large Scale Simulation Program (No. 13/14-4, 14/15-10).

Appendix A: Zero-mode integral

In this appendix, we evaluate the U_0 integrals which are necessary for numerical estimation of $Z_M^{\rm 2pt}$ or $Z_M^{\rm 3pt}$. Although our analysis in this paper is done only in the unquenched QCD, we use the partially quenched results by [25, 26], because some expressions are simpler for the partially quenched results, and the results would be easily extended to the partially quenched study in these expressions. The unquenched results are obtained simply by setting the valence quark mass m_v to the one of the sea quark masses.

We start with the so-called graded partition function which consists of n bosons and m fermions. Its non-perturbative analytic form is given by [25, 26]

$$\mathcal{Z}^Q_{n,m}(\{\mu_i\}) \;=\; \frac{\det[\mu_i^{j-1}\mathcal{J}_{Q+j-1}(\mu_i)]_{i,j=1,\cdots n+m}}{\prod_{j>i=1}^{n}(\mu_j^2-\mu_i^2)\prod_{j>i=n+1}^{n+m}(\mu_j^2-\mu_i^2)}, \tag{A1}$$

in a fixed topological sector of Q. Here $\mathcal{J}$'s are defined as $\mathcal{J}_{Q+j-1}(\mu_i) \equiv (-1)^{j-1}K_{Q+j-1}(\mu_i)$ for $i=1,\cdots n$ and $\mathcal{J}_{Q+j-1}(\mu_i) \equiv I_{Q+j-1}(\mu_i)$ for $i=n+1,\cdots n+m$, where K_ν and I_ν are the modified Bessel functions. Partial quenching is completed by taking the boson masses to those of valence fermions.

Integrals of some diagonal matrix elements are obtained by simply differentiating the partition function,

$$\begin{aligned}
\mathcal{S}_v \;&\equiv\; \frac{1}{2}\left\langle [U_0]_{vv}+[U_0^\dagger]_{vv}\right\rangle_{U_0} \;=\; \lim_{\mu_b\to\mu_v}\frac{\partial}{\partial\mu_v}\ln\mathcal{Z}^Q_{1,1+N_f}\left(\mu_b,\mu_v,\{\mu_{sea}\}\right),\\
\mathcal{D}_v \;&\equiv\; \frac{1}{4}\left\langle \left([U_0]_{vv}+[U_0^\dagger]_{vv}\right)^2\right\rangle_{U_0}\\
&=\; \frac{1}{\mathcal{Z}^Q_{N_f}(\{\mu_{sea}\})}\lim_{\mu_b\to\mu_v}\frac{\partial^2}{\partial\mu_v^2}\mathcal{Z}^Q_{1,1+N_f}\left(\mu_b,\mu_v,\{\mu_{sea}\}\right),\\
\mathcal{D}_{v_1v_2} \;&\equiv\; \frac{1}{4}\left\langle \left([U_0]_{v_1v_1}+[U_0^\dagger]_{v_1v_1}\right)\left([U_0]_{v_2v_2}+[U_0^\dagger]_{v_2v_2}\right)\right\rangle_{U_0}\\
&=\; \frac{1}{\mathcal{Z}^Q_{N_f}(\{\mu_{sea}\})}\lim_{\mu_{b_1}\to\mu_{v_1},\mu_{b_2}\to\mu_{v_2}}\frac{\partial}{\partial\mu_{v_1}}\frac{\partial}{\partial\mu_{v_2}}\mathcal{Z}^Q_{2,2+N_f}\left(\mu_{b_1},\mu_{b_2},\mu_{v_1},\mu_{v_2},\{\mu_{sea}\}\right),
\end{aligned} \tag{A2}$$

and

$$\begin{aligned}
\mathcal{T}_{v_1v_2} \;&\equiv\; \frac{1}{8}\left\langle \left([U_0]_{v_1v_1}+[U_0^\dagger]_{v_1v_1}\right)^2\left([U_0]_{v_2v_2}+[U_0^\dagger]_{v_2v_2}\right)\right\rangle_{U_0}\\
&=\; \frac{1}{\mathcal{Z}^Q_{N_f}(\{\mu_{sea}\})}\lim_{\mu_{b_1}\to\mu_{v_1},\mu_{b_2}\to\mu_{v_2}}\frac{\partial^2}{\partial\mu_{v_1}}\frac{\partial}{\partial\mu_{v_2}}\mathcal{Z}^Q_{2,2+N_f}\left(\mu_{b_1},\mu_{b_2},\mu_{v_1},\mu_{v_2},\{\mu_{sea}\}\right).
\end{aligned} \tag{A3}$$

Then, U_0 integrals for the degenerate case $m_1 = m_2$ can be written as

$$\langle \mathcal{B}(U_0) \rangle = 2\left[1 + \frac{Q^2}{\mu_1} - \frac{2}{N_f}\mathcal{D}_1 + \left(1 + \frac{2}{N_f}\right)\mathcal{D}_{11}\right], \tag{A4}$$

$$\left\langle \mathcal{D}^0(U_0) \right\rangle_{U_0} = 4\mathcal{S}_1, \tag{A5}$$

$$\left\langle \mathcal{D}^1(U_0) \right\rangle_{U_0} = \frac{N_f}{\mu_1}\left(1 - \mathcal{D}_{11} - \frac{Q^2}{\mu_1^2}\right), \tag{A6}$$

$$\left\langle \mathcal{D}^2(U_0) \right\rangle_{U_0} = -\frac{2}{\mu_1}\left(\partial_1\mathcal{S}_1 - \frac{\mathcal{S}_1}{\mu_1} - \frac{2Q^2}{\mu_1}\mathcal{S}_1\right), \tag{A7}$$

$$\left\langle \mathcal{D}^3(U_0) \right\rangle_{U_0} = -\frac{4}{\mu_1}\left(\frac{1}{N_f} - \frac{\mathcal{D}_{11}}{N_f} - \frac{3Q^2}{N_f\mu_1^2} - \partial_1\mathcal{S}_1\right), \tag{A8}$$

$$\left\langle \mathcal{D}^4(U_0) \right\rangle_{U_0} = \frac{4}{N_f^2}\partial_1\mathcal{D}_1 + \frac{2}{\mu_1}\partial_1\mathcal{S}_1 + \frac{4(N_f-2)}{N_f^2}\partial_1\mathcal{D}_{1j}|_{m_j=m_1},$$

$$\left\langle \mathcal{E}(U_0) \right\rangle_{U_0} = 2\left(1 + 3\mathcal{D}_{11} + \frac{Q^2}{\mu_1^2}\right), \tag{A9}$$

$$\begin{aligned}\left\langle \mathcal{G}(U_0) \right\rangle_{U_0} = 2\Bigg[&\mathcal{T}_{11} - \frac{\partial_1\mathcal{D}_1}{2} - \frac{3\mathcal{D}_1}{2\mu_1} + \left(-3 + \frac{-4N_f+3}{2\mu_1}\right)\mathcal{D}_{11} \\ &+ \left(3 + \frac{3}{2\mu_1^2} + \frac{3Q^2}{\mu_1^2}\right)\mathcal{S}_1 - 1 - \frac{Q^2}{\mu_1^2}\left(1 + \frac{N_f}{\mu_1}\right)\Bigg],\end{aligned} \tag{A10}$$

$$\left\langle \mathcal{H}(U_0) \right\rangle_{U_0} = -4\left[\frac{1 - \mathcal{D}_{11}}{2N_f\mu_1} - \frac{\partial_1\mathcal{S}_1}{\mu_1} - \frac{3Q^2}{2\mu_1^3 N_f}\right], \tag{A11}$$

Here, we have used

$$\lim_{\mu_1\to\mu_2}\frac{\mathcal{S}_1 - \mathcal{S}_2}{\mu_1 - \mu_2} = \partial_1\mathcal{S}_1 \tag{A12}$$

Note that the derivative ∂_v is taken w.r.t the valence degree of freedom *after* $\mu_b = \mu_v$ limit is taken. This partially quenched expression is simpler than that of unquenched theory, as shown in Ref. [33].

It is also useful to note

$$\mathcal{D}_{11} \equiv \lim_{\mu_2\to\mu_1}\mathcal{D}_{12} = -\left.\frac{1}{\mathcal{Z}^Q_{0,N_f}(\mu_{sea})}\frac{\partial}{\partial\mu_b}\frac{\partial}{\partial\mu_v}\mathcal{Z}^Q_{1,1+N_f}(\mu_b,\mu_v,\{\mu_{sea}\})\right|_{\mu_b=\mu_v=\mu_1}, \tag{A13}$$

which was shown in Appendix of Ref [20]. With this, the following non-trivial relations are obtained,

$$\partial_1\mathcal{S}_1 = \mathcal{D}_1 - \mathcal{D}_{11}, \quad \partial_1^2\mathcal{S}_1 = \partial_1\mathcal{D}_1 - 2\partial_1\mathcal{D}_{12}|_{m_2=m_1}. \tag{A14}$$

Similarly, we can use

$$\mathcal{T}_{11} \equiv \lim_{\mu_2\to\mu_1}\mathcal{T}_{21} = -\left.\frac{1}{\mathcal{Z}^Q_{0,N_f}(\mu_{sea})}\frac{\partial}{\partial\mu_b}\frac{\partial^2}{\partial^2\mu_v}\mathcal{Z}^Q_{1,1+N_f}(\mu_b,\mu_v,\{\mu_{sea}\})\right|_{\mu_b=\mu_v=\mu_1}. \tag{A15}$$

Appendix B: Loop momentum summations

In the calculation of the one-loop diagram, we have encountered the momentum summation:

$$I_{\mu\nu}(q_0, \mathbf{q}) \;=\; \frac{1}{V}\sum_{p\neq 0,q} \frac{p^\mu(q^\nu - 2p^\nu)}{p^2(q-p)^2} \quad (q^2 = q_0^2 + \mathbf{q}^2). \tag{B1}$$

From the symmetry, on a finite volume $V = TL^3$ we can decompose it as

$$I_{\mu\nu}(q_0, \mathbf{q}) \;=\; \delta_{\mu\nu} I_1(q_0, \mathbf{q}) + \delta_{\mu 0}\delta_{\nu 0} I_2(q_0, \mathbf{q}) + q_\mu q_\nu I_3(q_0, \mathbf{q}). \tag{B2}$$

Note that another possible choice $\sum_{i=1}^3 \delta_{\mu i}\delta_{\nu i}$ is not independent from the others since $\delta_{\mu\nu} = \delta_{\mu 0}\delta_{\nu 0} + \sum_{i=1}^3 \delta_{\mu i}\delta_{\nu i}$.

For a vector $\bar{q}_\mu$ which satisfy $q \cdot \bar{q} = 0$, we can simplify

$$I_{\mu\nu}(q_0, \mathbf{q})\bar{q}^\nu \;=\; \bar{q}_\mu I_1(q_0, \mathbf{q}) + \delta_{\mu 0}\bar{q}_0 I_2(q_0, \mathbf{q}). \tag{B3}$$

In particular, it is useful to note

$$I_{0\nu}(q_0, \mathbf{q})\bar{q}^\nu \;=\; \bar{q}_0 l(q_0, \mathbf{q}), \tag{B4}$$

where

$$l(q_0, \mathbf{q}) \;\equiv\; I_1(q_0, \mathbf{q}) + I_2(q_0, \mathbf{q}). \tag{B5}$$

---

[1] H. Fukaya and T. Suzuki, Phys. Rev. D **90**, no. 11, 114508 (2014) doi:10.1103/PhysRevD.90.114508 [arXiv:1409.0327 [hep-lat]].

[2] H. Fukaya and T. Suzuki, PoS LATTICE **2013**, 114 (2014) [arXiv:1402.2722 [hep-lat]].

[3] N. Cabibbo, Phys. Rev. Lett. **10**, 531 (1963).

[4] M. Kobayashi and T. Maskawa, Prog. Theor. Phys. **49**, 652 (1973).

[5] S. Aoki *et al.*, Eur. Phys. J. C **74**, 2890 (2014) [arXiv:1310.8555 [hep-lat]].

[6] J. Gasser and H. Leutwyler, Phys. Lett. B **184**, 83 (1987). doi:10.1016/0370-2693(87)90492-8

[7] J. Gasser and H. Leutwyler, Nucl. Phys. B **307**, 763 (1988). doi:10.1016/0550-3213(88)90107-1

[8] J. Gasser and H. Leutwyler, Annals Phys. **158**, 142 (1984);

[9] J. Gasser and H. Leutwyler, Nucl. Phys. B **250**, 465 (1985).

[10] K. A. Olive *et al.* [Particle Data Group Collaboration], Chin. Phys. C **38**, 090001 (2014).

[11] B. B. Brandt, Int. J. Mod. Phys. E **22**, 1330030 (2013) [arXiv:1310.6389 [hep-lat]].

[12] J. Koponen *et al.*, arXiv:1311.3513 [hep-lat].

[13] H. Fukaya *et al.*, (JLQCD Collaboration), arXiv:1211.0743 [hep-lat].

[14] H. Fukaya, S. Aoki, S. Hashimoto, T. Kaneko, H. Matsufuru and J. Noaki, Phys. Rev. D **90**, 034506 (2014) [arXiv:1405.4077 [hep-lat]].

[15] M. Kieburg, J. J. M. Verbaarschot and S. Zafeiropoulos, Phys. Rev. D **88**, 094502 (2013) [arXiv:1307.7251 [hep-lat]].

[16] F. C. Hansen, Nucl. Phys. B **345**, 685 (1990).

[17] F. C. Hansen and H. Leutwyler, Nucl. Phys. B **350**, 201 (1991).

[18] L. Giusti, P. Hernandez, M. Laine, P. Weisz and H. Wittig, JHEP **0411**, 016 (2004) [hep-lat/0407007].

[19] F. Bernardoni, P. H. Damgaard, H. Fukaya and P. Hernandez, JHEP **0810**, 008 (2008) [arXiv:0808.1986 [hep-lat]].

[20] S. Aoki and H. Fukaya, Phys. Rev. D **84**, 014501 (2011) [arXiv:1105.1606 [hep-lat]].

[21] G. Akemann and F. Pucci, PoS LATTICE **2012**, 264 (2012) [arXiv:1212.4061 [hep-lat]].

[22] P. Hernandez and M. Laine, JHEP **0301**, 063 (2003) [hep-lat/0212014].

[23] P. Hernandez, M. Laine, C. Pena, E. Torro, J. Wennekers and H. Wittig, JHEP **0805**, 043 (2008) [arXiv:0802.3591 [hep-lat]].

[24] H. Leutwyler and A. V. Smilga, Phys. Rev. D **46**, 5607 (1992).

[25] K. Splittorff and J. J. M. Verbaarschot, Phys. Rev. Lett. **90**, 041601 (2003).

[26] Y. V. Fyodorov and G. Akemann, JETP Lett. **77**, 438 (2003).

[27] S. Aoki *et al.* [JLQCD and TWQCD Collaboration], Phys. Rev. D **80**, 034508 (2009).

[28] T. Kaneko *et al.*[JLQCD Collaboration], PoS **LATTICE2010**, 146 (2010).

[29] F. Bernardoni and P. Hernandez, JHEP **0710**, 033 (2007) [arXiv:0707.3887 [hep-lat]].

[30] S. Aoki and H. Fukaya, Phys. Rev. D **81**, 034022 (2010) [arXiv:0906.4852 [hep-lat]].

[31] C. Bernard [MILC Collaboration], Phys. Rev. D **65**, 054031 (2002) [arXiv:hep-lat/0111051].

[32] P. Hasenfratz and H. Leutwyler, Nucl. Phys. B **343**, 241 (1990).

[33] P. H. Damgaard and H. Fukaya, Nucl. Phys. B **793**, 160 (2008) [arXiv:0707.3740 [hep-lat]].

[34] P. A. Boyle, J. M. Flynn, A. Juttner, C. Kelly, H. P. de Lima, C. M. Maynard, C. T. Sachra-

jda and J. M. Zanotti, JHEP **0807**, 112 (2008) doi:10.1088/1126-6708/2008/07/112 [arXiv:0804.3971 [hep-lat]].

[35] J. Bijnens and P. Talavera, JHEP **0203**, 046 (2002) doi:10.1088/1126-6708/2002/03/046 [hep-ph/0203049].

[36] T. Mehen and B. C. Tiburzi, Phys. Rev. D **72**, 014501 (2005) [hep-lat/0505014].

[37] B. C. Tiburzi, arXiv:1407.4059 [hep-lat].

[38] H. Na, C. T. H. Davies, E. Follana, J. Koponen, G. P. Lepage and J. Shigemitsu, Phys. Rev. D **84**, 114505 (2011) doi:10.1103/PhysRevD.84.114505 [arXiv:1109.1501 [hep-lat]].

[39] J. Koponen, C. T. H. Davies, G. C. Donald, E. Follana, G. P. Lepage, H. Na and J. Shigemitsu, arXiv:1305.1462 [hep-lat].

[40] T. Primer *et al.* [LATTICE-FERMILAB and LATTICE-MILC Collaborations], arXiv:1511.04000 [hep-lat].

[41] N. Carrasco, P. Lami, V. Lubicz, E. Picca, L. Riggio, S. Simula and C. Tarantino, arXiv:1511.04877 [hep-lat].

[42] Y. Amhis *et al.* [Heavy Flavor Averaging Group (HFAG) Collaboration], arXiv:1412.7515 [hep-ex].

[43] P. A. Boyle, J. M. Flynn, A. Juttner, C. T. Sachrajda and J. M. Zanotti, JHEP **0705**, 016 (2007) doi:10.1088/1126-6708/2007/05/016 [hep-lat/0703005 [HEP-LAT]].

[44] D. Besson *et al.* [CLEO Collaboration], Phys. Rev. D **80**, 032005 (2009) [arXiv:0906.2983 [hep-ex]].

[45] B. Aubert *et al.* [BaBar Collaboration], Phys. Rev. D **76**, 052005 (2007) [arXiv:0704.0020 [hep-ex]].

[46] L. Widhalm *et al.* [Belle Collaboration], Phys. Rev. Lett. **97**, 061804 (2006) [hep-ex/0604049].

[47] M. Tomii *et al.* [JLQCD Collaboration], arXiv:1511.09170 [hep-lat].

[48] B. Fahy, G. Cossu, S. Hashimoto, T. Kaneko, J. Noaki, and M. Tomii [JLQCD Collaboration], PoS (LATTICE 2015) 074.

[49] H. Na, C. T. H. Davies, E. Follana, G. P. Lepage and J. Shigemitsu, Phys. Rev. D **82**, 114506 (2010) doi:10.1103/PhysRevD.82.114506 [arXiv:1008.4562 [hep-lat]].

[50] Y. Nambu, Phys. Rev. **106**, 1366 (1957). doi:10.1103/PhysRev.106.1366

[51] W. R. Frazer and J. R. Fulco, Phys. Rev. **117**, 1609 (1960). doi:10.1103/PhysRev.117.1609

[52] J. J. Sakurai, Annals Phys. **11**, 1 (1960). doi:10.1016/0003-4916(60)90126-3

[53] M. Gell-Mann, Phys. Rev. **125**, 1067 (1962). doi:10.1103/PhysRev.125.1067

[54] M. Gell-Mann and F. Zachariasen, Phys. Rev. **124**, 953 (1961). doi:10.1103/PhysRev.124.953

[55] M. Gell-Mann, D. Sharp and W. G. Wagner, Phys. Rev. Lett. **8**, 261 (1962). doi:10.1103/PhysRevLett.8.261

[56] C. G. Boyd, B. Grinstein and R. F. Lebed, Phys. Lett. B **353**, 306 (1995) doi:10.1016/0370-2693(95)00480-9 [hep-ph/9504235].